Understanding and Enhancing Message Passing on Heterophilic Graphs via Compatibility Matrix

Zhuonan Zheng[★♠], **Yuanchen Bei**[♠], **Zhiyao Zhou**[♠], **Sheng Zhou**[★‡*],
Yao Ma[†], **Ming Gu**[★♠], **Hongjia Xu**[★♠], **Jiawei Chen**[♠], **Jiajun Bu**[★♠]
[★] Zhejiang Key Laboratory of Accessible Perception and Intelligent Systems, Zhejiang University
[♠]College of Computer Science and Technology, Zhejiang University
[‡]School of Software Technology, Zhejiang University
[†] School of Science, Rensselaer Polytechnic Institute

Abstract

Graph Neural Networks (GNNs) excel in graph mining tasks thanks to their message-passing mechanism, which aligns with the homophily assumption. However, connected nodes can also exhibit inconsistent behaviors, termed *heterophilic* patterns, sparking interest in heterophilic GNNs (HTGNNs). Although the message-passing mechanism seems unsuitable for heterophilic graphs owing to the propagation of dissimilar messages, it is still popular in HTGNNs and consistently achieves notable success. Some efforts have investigated such an interesting phenomenon, but are limited in the *data* perspective. The *model*-perspective understanding remains largely unexplored, which is conducive to guiding the designs of HTGNNs. To fill this gap, we build the connection between node discriminability and the compatibility matrix (CM). We reveal that the effectiveness of the message passing in HTGNNs may be credited to increasing the proposed *Compatibility Matrix Discriminability (CMD)*. However, the issues of sparsity and noise pose great challenges to leveraging CM. Thus, we propose CMGNN, a novel approach to alleviate these issues while enhancing the CM and node embeddings explicitly. A thorough evaluation involving 13 datasets and comparison against 20 well-established baselines highlights the superiority of CMGNN.

1 Introduction

Graph Neural Networks (GNNs) have shown remarkable performance in graph mining tasks, such as social network analysis [1, 2] and recommender systems [3, 4]. The widely used message-passing mechanism is typically based on the homophily assumption [5], which assumes that nodes are inclined to behave similarly to their neighbors [6]. However, this assumption is often violated in real-world graphs, where connected nodes exhibit a contrasting tendency called *heterophily* [7]. In response to the challenges of heterophily, *heterophilic GNNs (HTGNNs)* have attracted considerable interest [6, 8, 9], with numerous innovative approaches [10–13]. However, the majority of them continue to employ a message-passing mechanism and remain successful, which was not originally designed for heterophilic graphs, as they tend to incorporate excessive messages from disparate classes. This raises a question: *Why does message passing remain effective on heterophilic graphs?*

Some efforts [6, 9, 14, 15] have begun to investigate this question and reveal that vanilla message-passing (VMP) can still work on heterophilic graphs under certain conditions. However, these works are limited in studying what kind of data is suitable for VMP. A large part of HTGNNs have modified the message-passing mechanism in response to heterophily, namely heterophilic message-passing (HTMP), which outperforms VMP on heterophilic graphs. *How HTMP works effectively in*

[*] Corresponding Author: zhousheng_zju@zju.edu.cn.

39th Conference on Neural Information Processing Systems (NeurIPS 2025).

certain data remains largely unexplored. In this paper, we investigate the connection between node discriminability and the compatibility matrix (CM), that is, the latent connection preference among classes within a graph. We propose the Compatibility Matrix Discriminability (CMD) to measure the discriminability of CM. Theoretical and empirical analyses prove that node discriminability and CMD are positively correlated in VMP while ignoring the influence of node degrees. In addition, a toy example and a posterior evaluation in representative HTGNN show that *the effectiveness of existing HTMP mechanisms may be attributed to increasing CMD*, which leads to better node embeddings.

This discovery explains the essence of HTMP and provides insight for the design of new HTGNNs. Nevertheless, the graph *sparsity* and *noise* bring significant challenges for leveraging the CM as they can cause low-quality CM estimations, misguiding the message passing. To fill this gap, we propose a novel Compatibility Matrix-aware Graph Neural Network (CMGNN), which alleviates the sparsity and noise issues by introducing supplementary CM-aware messages while preserving the original neighborhood information. Meanwhile, a targeted constraint is applied to explicitly and simultaneously enhance the CMD and node embeddings. We then conduct fair comparisons to evaluate the effectiveness of CMGNN, compared with 20 baseline methods on 13 datasets with varying homophily levels and scales. Extensive experimental results demonstrate that CMGNN outperforms all baseline methods on heterophilic graphs while also being competitive on homophilic graphs. The contributions of this paper are summarized as follows:

- **Theoretical Findings**. We reveal the possible principle behind the heterophilic message-passing mechanism through comprehensive theoretical and empirical analyses, which may help people better understand the HTMP mechanism.
- **Proposed Method**. We introduce CMGNN, a novel approach that leverages and enhances the CM to learn better node embeddings while alleviating the issues of graph sparsity and noise.
- **Benchmarking and Evaluation**. We construct a comprehensive and fair benchmark to evaluate the effectiveness of CMGNN. Extensive experimental results show the superiority of CMGNN. Our code is available at https://github.com/zfx233/CMGNN.

2 Preliminaries

Notations. Given a graph $\mathcal{G} = (\mathcal{V}, \mathcal{E}, \mathbf{X}, \mathbf{A}, \mathbf{Y})$, $\mathcal{V}$ is the node set and $\mathcal{E}$ is the edge set. Nodes are characterized by the feature matrix $\mathbf{X} \in \mathbb{R}^{N \times d_f}$, where $N = |\mathcal{V}|$ denotes the number of nodes, d_f is the feature dimension. $\mathbf{Y} \in \mathbb{R}^{N \times 1}$ is the node labels with the one-hot version $\mathbf{C} \in \mathbb{R}^{N \times K}$, where K is the number of node classes. $\mathbf{A} \in \mathbb{R}^{N \times N}$ is the adjacency matrix, each element a_{ij} in $\mathbf{A}$ denotes whether there is an edge between i and j, and $\mathbf{D} = \text{diag}(d_1, ..., d_n)$ represents the diagonal degree matrix, where $d_i = \sum_j a_{ij}$. The normalized adjacency matrix is denoted by $\hat{\mathbf{A}} = \mathbf{D}^{-1}\mathbf{A}$. We use $\mathbf{1}$ to represent a matrix with all elements equal to 1.

Homophily and Heterophily. Graphs exhibit high homophily when a large fraction of neighboring nodes have the same labels as the central nodes, whereas graphs with high heterophily show the contrary. For measuring the homophily level, two widely used metrics are edge homophily h^e [16] and node homophily h^n [17], defined as $h^e = \frac{|\{e_{uv} | e_{uv} \in \mathcal{E},\ \mathbf{Y}_u = \mathbf{Y}_v\}|}{|\mathcal{E}|}$ and $h^n = \frac{1}{|\mathcal{V}|} \sum_{v \in \mathcal{V}} \frac{|\{u | e_{uv} \in \mathcal{E},\ \mathbf{Y}_u = \mathbf{Y}_v\}|}{\mathbf{d}_v}$. Both metrics range from $[0, 1]$, with higher values denoting greater homophily and lower values signifying stronger heterophily.

Vanilla Message-Passing (VMP). The vanilla message-passing mechanism plays a pivotal role in transforming and updating node embeddings based on the neighborhood [18]. Typically, the mechanism operates iteratively and comprises two stages:

$$\widetilde{\mathbf{Z}}^l = \text{AGGREGATE}(\mathbf{A}, \mathbf{Z}^{l-1}), \quad \mathbf{Z}^l = \text{COMBINE}\left(\mathbf{Z}^{l-1}, \widetilde{\mathbf{Z}}^l\right), \tag{1}$$

where the AGGREGATE function first aggregates the input messages $\mathbf{Z}^{l-1}$ from neighborhood $\mathbf{A}$ into $\widetilde{\mathbf{Z}}^l$, and subsequently, the COMBINE function combines the messages of the node ego and neighborhood aggregation, resulting in updated embeddings $\mathbf{Z}^l$.

Heterophilic Message-Passing (HTMP). To adapt to heterophily, many heterophilic message-passing methods have been proposed, which usually extend the neighborhood variously, enriching the sources of messages. In addition, the aggregation weights and the COMBINE function are often redesigned to collect neighbor messages preferentially while preserving the ego messages. Moreover, there may exist multiple messages collected from different neighborhoods in HTMP, which simultaneously form node embeddings. In this paper, we use "HTMP" methods to refer to the heterophilic GNNs that follow the message-passing mechanism. More detailed related works are available in Appendix A.

3 Exploring the Essence of Message Passing on Heterophilic Graphs

In this section, we aim to uncover the underlying principle that explains the effectiveness of HTMP Inspired by the key factors identified by Zhu et al. [9], we consider the compatibility matrix (CM) [7] as a potential path. To formally explore the connection between node discriminability and CM in message passing, we use the Expected Negative KL-divergence (ENKL) [15] to measure node discriminability and define Compatibility Matrix Discriminability (CMD) for CM.

Expected Negative KL-divergence (ENKL) [15]. ENKL can measure the inter-class node discriminability in the graph generated by the Contextual Stochastic Block Model for Homophily/Heterophily (CSBM-H) [15], a variation of the generative model CSBM [19], which has been widely adopted to study the behavior of GNNs [6, 20, 21]. In CSBM-H, the generated graph comprises two disjoint node sets, $i \in \mathcal{C}_0$ and $j \in \mathcal{C}_1$, representing two classes. The node features are generated independently, where x_i is generated from $N(\boldsymbol{\mu}_0, \sigma_0^2 \mathbf{I})$ and x_j from $N(\boldsymbol{\mu}_1, \sigma_1^2 \mathbf{I})$, with $\boldsymbol{\mu}_0, \boldsymbol{\mu}_1 \in \mathbb{R}^{F_h}$ and F_h as the embedding dimension. Node degrees for $\mathcal{C}_0$ and $\mathcal{C}_1$ are d_0, d_1 respectively. For $i \in \mathcal{C}_0$, its neighbors are independently sampled as $h \cdot d_0$ intra-class and $(1-h) \cdot d_0$ inter-class nodes, mirrored for $j \in \mathcal{C}_1$. Then, the ENKL is defined as follows:

$$\text{ENKL}(\mathbf{X}) = -d_{\mathbf{X}}^2\left(\frac{1}{4\sigma_1^2} + \frac{1}{4\sigma_0^2}\right) - \frac{F_h}{4}\left(\rho^2 + \frac{1}{\rho^2} - 2\right), \tag{2}$$

where $d_{\mathbf{X}}^2 = (\boldsymbol{\mu}_0 - \boldsymbol{\mu}_1)^T(\boldsymbol{\mu}_0 - \boldsymbol{\mu}_1)$, $\rho = \frac{\sigma_0}{\sigma_1}$. Different message-passing mechanisms can obtain different node embeddings with corresponding ENKL values, where smaller ENKL values correspond to more distinguishable node embeddings. Thus, ENKL can serve as a theoretically guaranteed evaluation criterion for different message passing approaches.

Compatibility Matrix (CM) [7]. CM characterizes the latent connection preference among classes within a graph. It is formatted as a matrix $\mathbf{M} \in \mathbb{R}^{K \times K}$, where the i-th row $\mathbf{M}_i$ denotes the connection probabilities between class i and all classes. It can be estimated empirically as follows:

$$\mathbf{M} = \text{Norm}(\mathbf{C}^T \mathbf{C}^{nb}), \quad \mathbf{C}^{nb} = \hat{\mathbf{A}}\mathbf{C}, \tag{3}$$

where Norm$(\cdot)$ is the L1 normalization for matrix row vectors and T is the matrix transpose operation. $\mathbf{C}^{nb} \in \mathbf{R}^{N \times K}$ is the *semantic neighborhoods* of nodes, indicating the proportion of neighbors from each class in the neighborhoods. Thus, the CM under CSBM-H settings is:

$$\mathbf{M}_{\text{CSBM-H}} = \begin{bmatrix} h, & 1-h \\ 1-h, & h \end{bmatrix}. \tag{4}$$

To measure the discriminability of CM, we define the Compatibility Matrix Discriminability (CMD).

Definition 3.1 (Compatibility Matrix Discriminability (CMD)). Given a compatibility matrix $\mathbf{M}$, the CMD is defined as the average L1 distance between rows (classes):

$$\text{CMD}(\mathbf{M}) = \frac{\sum_i^K \sum_{j \neq i}^K \|\mathbf{M}_i - \mathbf{M}_j\|_1}{K \cdot (K-1)}, \tag{5}$$

where K is the number of classes and $\mathbf{M}_i$ is the i-th row of $\mathbf{M}$. $\|\cdot\|_1$ denotes the L1 distance. The higher the CMD, the more distinguishable each row in the CM is.

We start with VMP to investigate the potential connection between CMD and ENKL. Following previous work [15], we use a low-pass (LP) operator $\hat{\mathbf{A}}$ as an example of VMP: $\mathbf{H}^{\text{LP}} = \hat{\mathbf{A}}\mathbf{X}$. Since all neighbors of each node share the same weight in VMP, CM can also indicate the proportion of class-level neighbor messages in node embeddings. Thus, discriminability in CM can be transferred to node embeddings in VMP. Formally, through theoretical analysis, we have the following theorem.

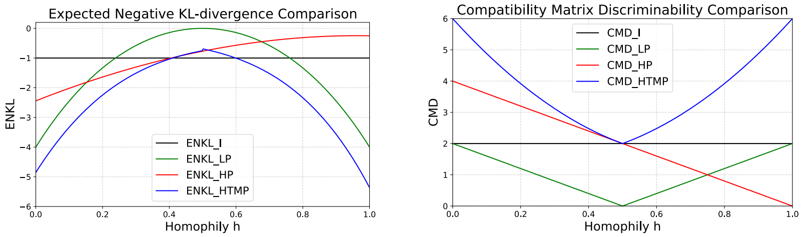

(a) ENKL (b) CMD

Figure 1: Visualization of CSBM-H ($\boldsymbol{\mu}_0 = [-1, 0], \boldsymbol{\mu}_1 = [0, 1], \sigma_0^2 = 1, \sigma_1^2 = 2, d_0 = 5, d_1 = 5$).

Theorem 3.2 (**Negatively Correlation between CMD and ENKL of VMP**). *Consider a graph $\mathcal{G} \sim$ CSBM-H$(\boldsymbol{\mu}_0, \boldsymbol{\mu}_1, \sigma_0^2 I, \sigma_1^2 I, d_0, d_1, h)$ and the LP operator $\hat{\mathbf{A}}$ as VMP. When ignoring the influence of node degrees, i.e., $d_0 = d_1$, we have $Cov(CMD(\mathbf{M}_{CSBM\text{-}H}), ENKL(\mathbf{H}^{LP})) < 0$, where $Cov(\cdot)$ denotes the covariance. It means that the CMD and ENKL of VMP are negatively correlated.*

The detailed proof is available in Appendix B. We visualize the changing trends of CMD and ENKL of VMP (LP) in Figure 1 , which does show a negative correlation. Thus, more discriminable CM can lead to better node embeddings in VMP. This gives the reason why VMP can work well in some heterophilic situations: *A CM with low homophily but high discriminability can also lead to high node discriminability in VMP.* We conduct experiments on the synthetic dataset to provide empirical analysis in Appendix C. This conclusion is similar to previous works [6, 9] that discuss heterophily from the perspective of **data**, since heterophily and CM are both characteristics of data. However, they lack the understanding from the perspective of the model, which is conducive to guiding the designs of HTGNNs. To fill this gap, we take a further step in understanding this theoretical finding with a **model** perspective and consider such a question: *when given the exact data, can we enhance the CMD through the model to learn better embeddings?* Coincidentally, this may able to explain the essence of HTMP methods, as the weights of practical class-level neighbor messages in these HTMP methods may be different from the original CM. Since CM is a fixed concept for describing the original data, we introduce Weighted-CM for the sake of distinction.

Definition 3.3 (**Weighted Compatibility Matrix (Weighted-CM)**). The weights of practical class-level neighbor messages after message passing. It is also formatted as a matrix $\tilde{\mathbf{M}} \in \mathbb{R}^{K \times K}$, where the i-th row $\tilde{\mathbf{M}}_i$ denotes the aggregate weights of all classes for class i. It can be estimated as follows:

$$\tilde{\mathbf{M}} = \mathbf{C}^T \dot{\mathbf{A}} \mathbf{C}, \tag{6}$$

where $\dot{\mathbf{A}} \in \mathbb{R}^{N \times N}$ is the practical aggregate weights matrix during message passing. Note that there is no strict limit to the values: $\tilde{m}_{ij} \in \mathbb{R}$.

For further analysis, we define the identity (I), high-pass (HP) and heterophilic message-pass (HTMP) operators as $\dot{\mathbf{A}}^{\text{I}} = \mathbf{I}$, $\dot{\mathbf{A}}^{\text{HP}} = \mathbf{I} - \hat{\mathbf{A}}$, and $\dot{\mathbf{A}}^{\text{HTMP}} = a\mathbf{I} + b\hat{\mathbf{A}} + c\hat{\mathbf{A}}^2$, where $a, b, c \in [-1, 1]$ are three learnable weight parameters. The high-pass operator can capture the difference between the central node and its neighborhoods in heterophilic graphs. The HTMP operator is a typical scheme that aims to utilize the linear combination of multiple-order neighborhood messages to obtain more distinguishable embeddings. The embedding matrices after message passing can be represented as $\mathbf{H}^{\text{o}} = \dot{\mathbf{A}}^{\text{o}}\mathbf{X}, \text{o} \in \{\text{I, LP, HP, HTMP}\}$. Thus, the Weighted-CMs and corresponding CMDs of identity, LP, HP, and HTMP operators are as follows:

$$\tilde{\mathbf{M}}^{\text{I}} = \begin{bmatrix} 1, & 0 \\ 0, & 1 \end{bmatrix}, \tilde{\mathbf{M}}^{\text{LP}} = \begin{bmatrix} h, & 1-h \\ 1-h, & h \end{bmatrix}, \tilde{\mathbf{M}}^{\text{HP}} = \begin{bmatrix} 1-h, & h-1 \\ h-1, & 1-h \end{bmatrix},$$
$$\tilde{\mathbf{M}}^{\text{HTMP}} = \begin{bmatrix} a + bh + c[h^2 + (1-h)^2], & b(1-h) + 2ch(1-h) \\ b(1-h) + 2ch(1-h), & a + bh + c[h^2 + (1-h)^2] \end{bmatrix}, \tag{7}$$
$$\text{CMD}^{\text{I}} = 2,\ \text{CMD}^{\text{LP}} = 4|h - \frac{1}{2}|,\ \text{CMD}^{\text{HP}} = 4|h - 1|,\ \text{CMD}^{\text{HTMP}} = 4|\frac{a}{2} + (h - \frac{1}{2})b + 2(h - \frac{1}{2})^2 c|.$$

Table 1: CMD and ENKL values of different operators on real-world graphs.

Dataset	**Roman-Empire**		**Amazon-Ratings**		**Chameleon-F**		**Squirrel-F**	
Operator	**CMD**	**ENKL**	**CMD**	**ENKL**	**CMD**	**ENKL**	**CMD**	**ENKL**
LP	0.85	-0.76	0.46	-0.26	0.27	-25.38	0.08	-14.84
HP	2.77	-2.62	1.95	-0.80	2.07	-126.5	2.02	-67.89
HTMP (Case 1)	3.31	-4.13	2.35	-1.14	2.39	-150.8	2.22	-80.05
HTMP (Case 2)	3.55	-5.04	3.10	-2.41	2.85	-170.6	2.28	-89.52

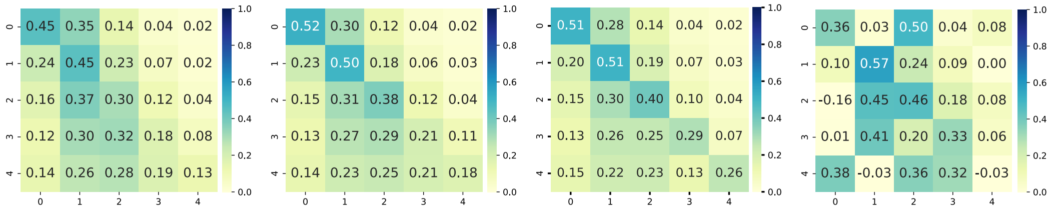

(a) Fixed(LP),CMD=0.46 (b) GloGNN,CMD=0.59 (c) GPR-GNN,CMD=0.62 (d) ACM-GCN,CMD=0.97

Figure 2: Visualizations of Weighted-CMs estimated through various methods on Amazon-Ratings.

Since we aim to obtain the largest CMD, the values of a, b, c can be set as follows:

$$\begin{aligned}
&\text{Case 1, } h \geq \frac{1}{2}: a = 1, b = 1, c = 1, \dot{\hat{\mathbf{A}}}^{\text{HTMP}} = \mathbf{I} + \hat{\mathbf{A}} + \hat{\mathbf{A}}^2, \text{CMD}^{\text{HTMP}} = 8(h - \frac{1}{4})^2 + \frac{3}{2}, \\
&\text{Case 2, } h < \frac{1}{2}: a = 1, b = -1, c = 1, \dot{\hat{\mathbf{A}}}^{\text{HTMP}} = \mathbf{I} - \hat{\mathbf{A}} + \hat{\mathbf{A}}^2, \text{CMD}^{\text{HTMP}} = 8(h - \frac{3}{4})^2 + \frac{3}{2}.
\end{aligned} \tag{8}$$

We visualize the changing trends of CMD and ENKL of the four operators in Figure 1. Similarly, the two changing trends are negatively correlated independently for each operator, which can also be proven by theoretical analysis. Although the relationship between the CMD and ENKL values among different operators is not consistent, we still show that *it is feasible to obtain better embeddings by increasing the CMD in HTMP as the HTMP operator achieves the minimum ENKL*, i.e., the best node discriminability, in most cases by different combinations of parameters a, b, c.

However, there are significant gaps between the theoretical assumptions of CSBM-H and real-world graphs, including multi-class, semi-supervised settings, imbalanced node degrees, and potential low-quality node features, among others. *What is the impact on the relationship between CMD and ENKL?* We count the values of ENKL and CMD when different operators are used on some real graphs, as in Table 1. We find that *the negative correlation between CMD and ENKL still holds on real-world graphs*, which expands the Theorem 3.2. In addition to the above analyses, we also investigated three representative methods, GloGNN [22], GPR-GNN [23], and ACM-GCN [12].

Observation 3.4 (**The increased CMDs of representative HTGNNs**). We conduct a posterior evaluation on the results of GloGNN, GPR-GNN, and ACM-GCN. All the CMDs of Weighted-CMs have been significantly improved compared to the fixed one of the original data, as shown in Figure 2.

More details and examples about the posterior evaluation can be found in Appendix D. The success of the HTMP operator and Observation 3.4 gives a possible answer to the effectiveness of HTMP:

Remark 3.5 (**Increasing CMD is a possible reason for the effectiveness of HTMP**). Given certain data, the HTMP mechanism can increase the CMD by replacing the fixed one with the Weighted-CM via various model-level designs, leading to better node embeddings.

This explains the underlying principle of HTMP and provides insight for designing new HTGNNs via increasing CMD. Several existing works [7, 24, 25] have naively estimated and used CM without increasing CMD. However, to make good use of CM, there are still two significant issues, namely sparsity and noise, when considering real-world heterophilic graphs. First, *node degrees can be very imbalanced*. Some nodes may have few neighbors due to the sparsity of the graph, which may not only show a highly inconsistent semantic neighborhood with CM but also be harmful to the effectiveness of message passing. Second, *node labels are not fully available* in the semi-supervised

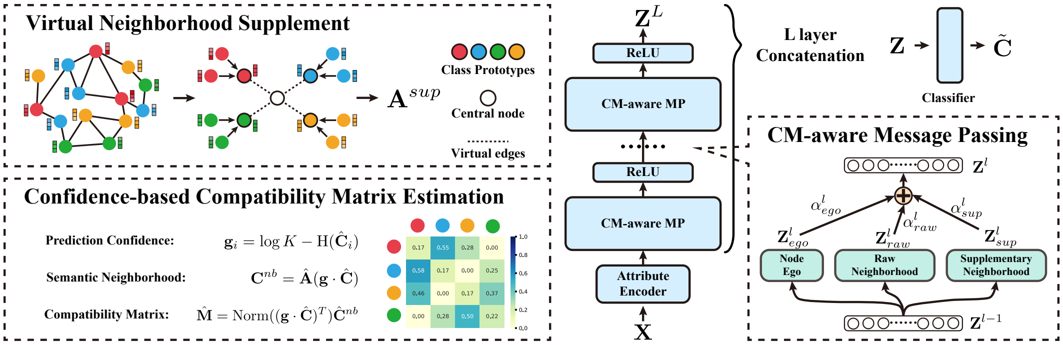

Figure 3: The overall framework of CMGNN.

setting. Inaccurate predictions of node labels can cause low-quality CM estimation, which misguides the message passing, leading to low-discriminative node embeddings. These issues pose significant challenges to the explicit modeling and effective utilization of CM.

4 Methodology

To address these issues, we introduce Compatibility Matrix-Aware GNN (CMGNN), as shown in Figure 3, which alleviates the sparsity and noise issues by *virtual neighborhood supplement*, *confidence-based compatibility matrix estimation*, and *CM-aware message passing*. Then, a straightforward constraint is applied to explicitly enhance the discriminability of CM and node embeddings.

Virtual Neighborhood Supplement. Given the graph sparsity, some nodes may have low degrees. Thus, CMGNN introduces an additional virtual neighborhood to provide nodes with supplemental messages from each class. The virtual neighborhood is the same for all nodes, which consists of K additional virtual neighbors: $\mathbf{A}^{sup} = \mathbf{1} \in \mathbb{R}^{N\times K}$. It ensures accessibility to the messages of all classes for each node. Specifically, these additional neighbors are K virtual nodes, designed as the class prototypes based on the training set labels. The attributes $\mathbf{X}^{ptt} \in \mathbb{R}^{K\times d_f}$, neighborhoods $\mathbf{A}^{ptt} \in \mathbb{R}^{K\times N}$ and labels $\mathbf{Y}^{ptt} \in \mathbb{R}^{K\times K}$ of prototypes are defined as follows:

$$\mathbf{X}^{ptt} = \mathrm{Norm}(\mathbf{C}_{train}{}^{T}\mathbf{X}_{train}),\ \mathbf{A}^{ptt} = \mathbf{0},\ \mathbf{Y}^{ptt} = \mathbf{I}, \tag{9}$$

where $\mathbf{C}_{train}$ and $\mathbf{X}_{train}$ are the one-hot labels and attributes of nodes in the training set. Utilizing class prototypes to construct virtual neighborhoods can provide each node with representative messages of all classes, which builds the basis for CM-aware message passing.

Confidence-based CM Estimation. The CM can be calculated via Eq 3 with full-available labels. However, label information is not entirely available in semi-supervised settings. Thus, we try to estimate the CM with the help of pseudo labels. To mitigate the impact of potentially incorrect pseudo labels predicted by the model, we introduce a confidence metric $\mathbf{g} \in \mathbb{R}^{N\times 1}$ derived from the information entropy, with high entropy indicating low confidence:

$$\mathbf{g}_i = \log K - \mathrm{H}(\hat{\mathbf{C}}_i) \in [0, \log K], \tag{10}$$

where $\mathrm{H}(p) = -\sum_i p_i \log(p_i)$ denotes the entropy, $\hat{\mathbf{C}} \in \mathbb{R}^{N\times K}$ is the soft pseudo labels composed of training labels $\mathbf{C}_{train}$ and model predictions $\tilde{\mathbf{C}}$:

$$\hat{\mathbf{C}}_i = \begin{cases} \mathbf{C}_{train,i}, & v_i \in \mathcal{V}_{train}, \\ \tilde{\mathbf{C}}_i, & \text{otherwise}, \end{cases} \tag{11}$$

where $\mathcal{V}_{train}$ is the training set. Then the semantic neighborhoods of the nodes are calculated considering the confidence: $\hat{\mathbf{C}}^{nb} = \mathrm{Norm}(\hat{\mathbf{A}}(\mathbf{g} \cdot \hat{\mathbf{C}})) \in \mathbb{R}^{N\times K}$. Finally, we can estimate the compatibility matrix $\hat{\mathbf{M}} \in \mathbb{R}^{K\times K}$ as follows:

$$\hat{\mathbf{M}} = \mathrm{Norm}((\mathbf{g} \cdot \hat{\mathbf{C}})^T)\hat{\mathbf{C}}^{nb}. \tag{12}$$

Note that the CM is repeatedly updated during training. To improve efficiency and stability, CM is not estimated in every epoch. It remains fixed until the evaluation performance improves.

CM-aware Message Passing. Relying entirely on CM to guide message passing can lead to confusing embeddings when the quality of CM is low. Therefore, we regard it as a separate supplementary message source while preserving the original neighborhood distribution. Specifically, CMGNN collects messages from node ego, raw neighborhoods $\mathbf{A}$ and the supplement neighborhoods $\mathbf{A}^{sup}$, respectively. The first two are widely used in HTGNNs as the ego-neighbor separation design principle [16], while the last provides a novel approach to apply CM. The messages from node ego and raw neighborhoods are obtained as follows:

$$\mathbf{Z}^l_{ego} = \mathbf{Z}^{l-1}\mathbf{W}^l_{ego},\ \ \mathbf{Z}^l_{raw} = \hat{\mathbf{A}}\mathbf{Z}^{l-1}\mathbf{W}^l_{raw}, \tag{13}$$

where $\mathbf{Z}^{l-1}$ is the input node embedding of layer l, $\mathbf{W}^l_{ego}, \mathbf{W}^l_{raw}$ are learnable matrices for message transformation. For the supplement neighborhood, we leverage CM to offer nodes additional messages personalized by their soft pseudo labels, which converts discriminability from CM into messages:

$$\mathbf{Z}^l_{sup} = (\mathbf{A}^{sup} \odot \hat{\mathbf{C}}\hat{\mathbf{M}})\mathbf{Z}^{l-1}_{ptt}\mathbf{W}^l_{sup}, \tag{14}$$

where $\odot$ is the Hadamard product, $\mathbf{Z}^{l-1}_{ptt}$ are the input embeddings of virtual prototype nodes obtained via the same message-passing process as real nodes. The aggregation weights $\hat{\mathbf{C}}\hat{\mathbf{M}}$ indicate the desired semantic neighborhoods of nodes, i.e., the desired class proportion of neighbors according to the class probability of central nodes. Using soft logits rather than one-hot pseudo labels preserves the real characteristics of nodes and reduces the impact of wrong predictions.

Given the diverse conditions of nodes, we apply adaptive weighted addition to combine these messages. Meanwhile, messages of multiple layers are concatenated to preserve information from different localities within the graph. The overall CM-aware message passing is described as follows:

$$\mathbf{Z}^l = \text{diag}(\alpha^l_{ego})\mathbf{Z}^l_{ego} + \text{diag}(\alpha^l_{raw})\mathbf{Z}^l_{raw} + \text{diag}(\alpha^l_{sup})\mathbf{Z}^l_{sup}, \quad \mathbf{Z} = \mathop{\Big\|}_{l=0}^{L} \mathbf{Z}^l, \tag{15}$$

where $\text{diag}(\alpha^l_{ego}), \text{diag}(\alpha^l_{raw}), \text{diag}(\alpha^l_{sup}) \in \mathbb{R}^{N\times 1}$ are the learnable combination weights, $\|$ denotes the concatenation operation, $\mathbf{Z}$ is the final node embeddings. The input embedding of the first layer is $\mathbf{Z}^0 = \mathbf{X}\mathbf{W}^0$ where $\mathbf{W}^0 \in \mathbb{R}^{d_f\times d_r}$ and d_r is the dimension of node emebddings. In practice, we use ReLU as the activation function between layers. Note that we use the prediction of the model $\tilde{\mathbf{C}}$ to estimate CM in the above process. It is initialized as a uniform distribution on each class and replaced by the output of CMGNN via a classifier CLA during the learning process:

$$\tilde{\mathbf{C}} = \text{CLA}(\mathbf{Z}). \tag{16}$$

Objective Function. As mentioned in Sec 3, enhancing the discriminability of CM is beneficial for learning better node embeddings. Thus, we introduce an additional discrimination loss $\mathcal{L}_{dis}$ to reduce the similarity of the desired neighborhood message among different classes, which simultaneously enhances the discriminability of CM and node embeddings. Experimental analysis in Section 5.4 demonstrates the effectiveness of this constraint to enhance the CM. The overall loss consists of a CrossEntropy loss $\mathcal{L}_{ce}$ and the discrimination loss $\mathcal{L}_{dis}$:

$$\mathcal{L} = \mathcal{L}_{ce}(\tilde{\mathbf{Z}}, \mathbf{Y}) + \lambda\mathcal{L}_{dis}, \quad \mathcal{L}_{dis} = \sum_{i\neq j} \text{Sim}(\hat{\mathbf{M}}_i\mathbf{Z}_{ptt}, \hat{\mathbf{M}}_j\mathbf{Z}_{ptt}), \tag{17}$$

where $\text{Sim}(\cdot)$ denotes the cosine similarity, $\mathbf{Z}_{ptt} \in \mathbb{R}^{K\times d_r}$ is the embeddings of virtual prototype nodes. More details of CMGNN including pseudo-code are available in Appendix E.

5 Experiments

5.1 Experimental Settings

As reported in Platonov et al. [26], some widely adopted datasets in existing works have critical drawbacks, leading to unreliable comparisons. Therefore, with a comprehensive review of existing benchmark evaluations, we construct a new collection of datasets and a unified codebase to fairly perform experimental evaluation. Specifically, we integrate 20 representative homophilic and heterophilic GNNs, construct a unified codebase, and evaluate their node classification performances on 13 datasets with various scales and heterophily levels.

Table 2: Node classification accuracy comparison (%). The error bar (±) denotes the standard deviation of results over 10 runs. The best and second-best results in each column are highlighted in **bold** font and underlined. OOM denotes out-of-memory error during training.

Dataset	Roman-Empire	Amazon-Ratings	Chameleon-F	Squirrel-F	Actor	Flickr	BlogCatalog	Pubmed	Avg. Rank
Homo.	0.05	0.38	0.25	0.22	0.22	0.24	0.4	0.8	
Nodes	22,662	24,492	890	2,223	7,600	7,575	5,196	19,717	
Edges	65,854	186,100	13,584	65,718	30,019	479,476	343,486	88,651	
Classes	18	5	5	5	5	9	6	3	
MLP	62.29 ± 1.03	42.66 ± 0.84	38.66 ± 4.02	36.74 ± 1.80	36.70 ± 0.85	89.82 ± 0.63	93.57 ± 0.55	87.48 ± 0.46	15.6
GCN	38.58 ± 2.35	45.00 ± 0.55	42.12 ± 3.82	37.89 ± 2.40	30.09 ± 0.74	68.33 ± 2.82	78.07 ± 1.17	87.66 ± 0.42	16.3
GAT	59.55 ± 1.45	47.72 ± 0.73	40.89 ± 3.50	38.22 ± 1.71	30.94 ± 0.95	57.22 ± 3.04	88.36 ± 1.37	87.45 ± 0.53	15.6
GraphSAGE	69.62 ± 1.40	45.07 ± 0.54	42.18 ± 4.64	38.13 ± 1.71	36.12 ± 1.40	92.00 ± 0.58	96.30 ± 0.44	88.86 ± 0.56	9.0
APPNP	70.77 ± 0.66	45.97 ± 0.49	42.07 ± 4.07	36.38 ± 1.20	34.86 ± 1.32	91.50 ± 0.51	96.29 ± 0.41	89.22 ± 0.58	10.9
GCNII	82.53 ± 0.37	47.53 ± 0.72	41.56 ± 4.15	40.70 ± 1.80	**37.51 ± 0.92**	91.64 ± 0.67	96.48 ± 0.62	89.96 ± 0.43	4.9
H2GCN	68.61 ± 1.05	37.20 ± 0.67	42.29 ± 4.57	35.82 ± 2.20	33.32 ± 0.90	91.25 ± 0.58	96.24 ± 0.39	89.32 ± 0.37	12.6
MixHop	79.06 ± 0.64	47.41 ± 1.00	44.97 ± 3.12	40.43 ± 1.40	36.99 ± 0.88	91.10 ± 0.46	96.22 ± 0.42	89.47 ± 0.35	6.6
GBK-GNN	66.04 ± 1.44	40.18 ± 1.94	41.73 ± 4.57	36.49 ± 1.37	35.91 ± 0.84	OOM	OOM	88.14 ± 0.43	16.5
GGCN	OOM	OOM	41.23 ± 4.08	36.76 ± 2.19	35.68 ± 0.87	90.84 ± 0.65	95.58 ± 0.44	89.04 ± 0.40	15.4
GloGNN	68.63 ± 0.63	48.62 ± 0.59	40.95 ± 5.95	36.85 ± 1.97	36.66 ± 0.81	90.47 ± 0.77	94.51 ± 0.49	89.60 ± 0.34	11.4
HOGGCN	OOM	OOM	43.35 ± 3.66	38.63 ± 1.95	36.47 ± 0.83	90.94 ± 0.72	94.75 ± 0.65	OOM	13.1
GPR-GNN	71.10 ± 0.66	46.87 ± 0.60	42.85 ± 3.48	37.66 ± 1.08	36.16 ± 1.02	91.20 ± 0.46	96.29 ± 0.44	89.26 ± 0.37	8.5
ACM-GCN	71.15 ± 0.73	50.64 ± 0.61	45.20 ± 4.14	40.90 ± 1.74	35.99 ± 1.44	91.43 ± 0.65	96.16 ± 0.57	89.94 ± 0.35	6.0
OrderedGNN	82.88 ± 0.71	51.15 ± 0.46	41.51 ± 4.15	36.94 ± 2.94	37.07 ± 0.95	91.43 ± 0.78	96.22 ± 0.35	**90.01 ± 0.35**	6.4
M2MGNN	83.97 ± 0.71	50.93 ± 0.45	40.39 ± 3.68	36.36 ± 3.06	35.92 ± 0.76	91.49 ± 0.76	96.34 ± 0.48	89.91 ± 0.35	8.8
N^2	80.42 ± 1.30	49.94 ± 0.86	42.46 ± 4.37	40.92 ± 2.25	35.51 ± 1.20	90.85 ± 0.78	96.22 ± 0.63	88.53 ± 0.50	8.5
CLP	67.36 ± 0.62	47.42 ± 0.44	41.73 ± 4.49	37.64 ± 1.37	36.67 ± 1.64	90.13 ± 0.67	94.45 ± 0.59	88.88 ± 0.42	11.8
EPFGNN	43.05 ± 0.40	45.16 ± 0.73	44.30 ± 3.91	40.47 ± 1.54	30.24 ± 1.14	57.54 ± 1.77	74.35 ± 2.22	87.06 ± 0.53	15.0
CPGNN	59.55 ± 0.84	46.65 ± 0.71	41.45 ± 4.84	37.24 ± 2.09	33.37 ± 1.02	80.46 ± 1.25	81.92 ± 1.06	87.98 ± 0.40	15.6
CMGNN	**84.35 ± 1.27**	**52.13 ± 0.55**	**45.70 ± 4.92**	**41.89 ± 2.34**	36.82 ± 0.78	**92.66 ± 0.46**	**97.00 ± 0.52**	89.99 ± 0.32	**1.5**

Table 3: Node classification accuracy (%) and time cost (minutes) comparison on large-scale graphs.

Dataset	Penn94		Twitch-Gamer		Genius		Pokec		Snap-Patents		Avg. Rank
Homo.	0.47		0.55		0.62		0.45		0.07		
Nodes	41,554		168,114		421,961		1,632,803		2,923,922		
Edges	1,362,229		6,797,557		984,979		30,622,564		13,975,788		
Classes	2		2		2		2		5		
Method	**Accuracy**	**Cost**	**Accuracy**	**Cost**	**Accuracy**	**Cost**	**Accuracy**	**Cost**	**Accuracy**	**Cost**	
MLP	74.71 ± 0.40	1	61.25 ± 0.19	1.5	82.54 ± 0.14	0.8	62.27 ± 0.08	48	31.50 ± 0.06	14	13.8
GCN	78.48 ± 0.41	2.7	61.30 ± 0.10	2.6	84.05 ± 0.12	1.6	70.17 ± 0.10	75	37.91 ± 0.06	35	9.4
GAT	77.94 ± 1.22	25	64.59 ± 0.20	103	82.01 ± 0.45	5	75.36 ± 0.18	243	38.38 ± 0.15	142	8.8
GraphSAGE	78.90 ± 0.37	2.8	62.14 ± 0.09	14	84.37 ± 0.15	4.1	77.22 ± 0.06	134	35.72 ± 0.12	125	7.8
APPNP	77.04 ± 0.35	4.5	60.28 ± 0.23	5.4	82.81 ± 0.29	4.7	62.01 ± 3.83	34	32.64 ± 0.07	57	13.4
GCNII	79.97 ± 0.40	14	64.97 ± 0.40	221	**86.45 ± 0.19**	89	77.75 ± 1.17	343	42.24 ± 0.68	495	3.4
MixHop	76.74 ± 1.17	8	62.25 ± 0.17	52	83.49 ± 0.27	10	76.97 ± 0.27	305	36.94 ± 0.17	152	8.6
GloGNN	82.29 ± 0.62	8	65.74 ± 0.20	163	84.54 ± 0.15	9.5	78.61 ± 0.79	263	34.27 ± 5.28	165	4.0
GPR-GNN	82.50 ± 0.32	9	61.03 ± 0.38	8	82.89 ± 0.64	4.4	75.45 ± 0.08	54	32.87 ± 0.10	39	9.2
ACM-GCN	80.67 ± 0.49	12	61.87 ± 0.71	58	80.63 ± 0.53	4.9	74.60 ± 0.46	393	37.53 ± 0.22	378	10.2
OrderedGNN	79.49 ± 0.86	14	64.55 ± 0.32	66	84.83 ± 0.75	31	75.79 ± 0.20	265	39.56 ± 0.34	385	5.4
M2MGNN	81.86 ± 0.24	74	OOM	/	84.43 ± 0.13	100	OOM	/	OOM	/	11.4
N^2	80.69 ± 0.44	35	**65.76 ± 0.19**	294	84.08 ± 1.40	538	OOM	/	OOM	/	8.8
CLP	74.62 ± 0.53	0.5	63.77 ± 0.18	1.7	82.51 ± 0.14	1.3	67.23 ± 0.10	13	32.05 ± 0.06	20	12.4
EPFGNN	72.53 ± 0.58	12	64.19 ± 0.23	21	81.99 ± 0.44	6.5	64.19 ± 0.23	93	OOM	/	13.4
CPGNN	78.20 ± 0.42	14	63.06 ± 0.25	15	80.70 ± 0.80	3.9	75.80 ± 0.11	123	37.09 ± 0.09	137	9.8
CMGNN	**83.01 ± 0.48**	17	65.18 ± 0.31	247	85.19 ± 0.53	20	**81.42 ± 0.55**	376	**59.86 ± 0.61**	69	**1.6**

Newly Organized Datasets. The newly organized datasets include (i) small-scale: Roman-Empire, Amazon-Ratings, Chameleon-F, Squirrel-F, Actor, Flickr, BlogCatalog and Pubmed; (ii) large-scale: Penn94, Twitch-Gamer, Genius, Pokec and Snap-Patents. Their statistics are summarized in Table 2 and Table 3. For consistency with existing methods, we randomly construct 10 splits with predefined proportions (48% / 32% / 20% for training / validation / test) for each dataset and report the mean accuracy and standard deviation of 10 splits.

Baseline Methods. For baseline methods, we choose 20 representative homophilic and heterophilic GNNs, including (i) shallow base model: MLP; (ii) homophilic GNNs: GCN [1], GAT [27], GraphSAGE [28], APPNP [29], GCNII [30]; (iii) heterophilic GNNs: H2GCN [16], MixHop [10], GBK-GNN [31], GGCN [32], GloGNN [22], HOGGCN [33], GPR-GNN [23], ACM-GCN [12], OrderedGNN [13], M2MGNN [34] and N^2 [35]; (iv) compatibility matrix-based methods: CLP [25], EPFGNN [24], CPGNN [7]. For each method, we integrate its code into a unified codebase and search for parameters in the space suggested by the original papers. All methods share the same call interfaces, ensuring a fair environment for comparison. More detailed descriptions about the drawbacks of previous datasets, newly organized datasets and other experimental settings can be found in Appendix F.

5.2 Performance Comparison

We evaluate the above methods and report their performances in Table 2 and Table 3.

Table 4: Ablation study results (%) between CMGNN and five ablation variants, where CE denotes the confidence-based CM estimation, SM denotes supplementary messages from the sufficient neighborhoods and DL denotes the discrimination loss.

Variants	Roman-Empire	Squirrel-F	Actor	Chameleon-F	Amazon-Ratings	Pokec	Penn94	Genius
CMGNN	**84.35 ± 1.27**	**41.89 ± 2.34**	**36.82 ± 0.78**	**45.70 ± 4.92**	**52.13 ± 0.55**	**81.42 ± 0.55**	**83.01 ± 0.48**	**85.19 ± 0.53**
W/O CE	83.88 ± 1.41	40.35 ± 2.43	36.47 ± 1.22	44.75 ± 3.05	51.93 ± 0.38	80.67 ± 0.65	82.58 ± 0.49	85.03 ± 0.47
W/O SM	83.82 ± 1.29	40.72 ± 2.28	36.05 ± 1.24	42.29 ± 4.38	51.91 ± 0.83	79.39 ± 0.37	81.68 ± 1.55	84.94 ± 0.56
W/O DL	83.63 ± 1.35	41.65 ± 2.55	36.41 ± 1.08	44.92 ± 4.12	52.05 ± 0.57	80.28 ± 0.49	81.34 ± 1.83	84.87 ± 0.75
W/O CE and DL	83.77 ± 1.38	39.80 ± 2.36	36.32 ± 1.05	44.58 ± 3.28	51.74 ± 0.55	79.26 ± 0.34	81.20 ± 0.61	84.53 ± 0.59
W/O SM and DL	83.48 ± 1.89	40.19 ± 2.69	35.66 ± 1.42	41.01 ± 3.09	51.49 ± 1.02	77.57 ± 0.44	80.71 ± 0.48	84.28 ± 0.50

Performance of Baselines. With the comprehensive benchmark, some interesting observations can be found. First, comparing MLP and *homophilic GNNs* , we find that VMP can still work well in Amazon-Ratings, Chameleon-F, and Squirrel-F, which meet the observations of previous works. Specifically, GCNII achieves an average rank of 4.9, which is even better than all HTGNNs. This may be attributed to the initial residual connection in GCNII, which enhances the practical Weighted-CM in message passing. As for *heterophilic GNNs*, they generally achieve better results than VMPs (GCN, GAT), demonstrating the effectiveness of their various designs for heterophily. Notably, MixHop, as an early method, can also achieve quite good performance. The previous SOTA methods, OrderedGNN and ACM-GCN, prove their effectiveness again through good rankings.

Performance of CMGNN. CMGNN achieves the best performance in 6 small-scale datasets with an average rank of 1.5, outperforming all baseline methods. This demonstrates the superiority of leveraging CM and increasing CMD while alleviating the sparsity and noise issues. Regarding the suboptimal performance in Actor, we speculate that this is because its node attributes and CM are not discriminative enough to provide valuable information via the supplementary messages, and are hard to enhance. On Pubmed, the raw identity-like CM is good enough, leading to a minor contribution from supplement messages. Despite this, CMGNN still achieves top-level performance.

Comparision with CM-based Methods. Some existing methods also utilize the CM to redefine pairwise relations (e.g., edge weights) for nodes. However, they suffer from the issues of sparsity and noise, as their performances and average ranks have significant gaps compared with CMGNN. In contrast, CMGNN leverages CM and virtual neighbors to construct supplementary messages while preserving the original neighborhood distribution, leading to the following advantages: (i) Better robustness for low-quality pseudo labels; (ii) Unlock the effectiveness of CM for low-degree nodes; (iii) More accurate estimation of CM. More detailed analyses are listed in Appendix G.1.

Performance on Large-Scale Graphs. To further evaluate the scalability of CMGNN, we also conduct experiments on five large-scale datasets. The performance and computational cost comparison are listed in Table 3. Again, CMGNN achieves superior performance with the best average rank of 1.6, while GCNII follows behind with a rank of 3.4. Meanwhile, CMGNN strikes a good balance between performance and efficiency, especially in Snap-Patents with 17% significant improvements and less time cost, demonstrating great scalability in handling of large-scale graphs.

Performance on Homophilic and Heterophilic Graphs. We divide all datasets into two groups according to their edge homophily levels with a threshold of 0.5. CMGNN shows significant effectiveness on heterophilic graphs with an average rank of 1.3 and achieves the best on 9 of 10 datasets. Also, CMGNN can keep competitive performance on homophilic graphs with an average rank of 2.3, which is also the best compared with baseline methods. Interestingly, some heterophilic GNNs work relatively better on homophilic graphs rather than heterophilic graphs, such as GloGNN and OrderedGNN. This might be because these methods are relatively more inclined to adapt to both situations.

5.3 Ablation Study

We conduct an ablation study on three key designs of CMGNN, including the confidence-based CM estimation (CE), supplementary messages from the virtual neighborhood (SM) and the discrimination loss (DL). The results are shown in Table 4. *Firstly*, all three components have indispensable contributions to CMGNN, as the absence of any part will degrade the performance. *Meanwhile*, the CE and DL have relatively small impacts while SM plays a more important role in most datasets. *Further*, we notice that CMGNN can reach a smaller standard deviation compared with the variants

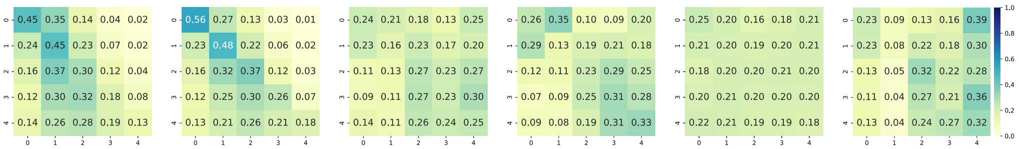

(a) Ama-O, 0.46 (b) Ama-W, 0.63 (c) Cha-O, 0.27 (d) Cha-W, 0.49 (e) Squ-O, 0.08 (f) Squ-W, 0.16

Figure 4: Visualizations of the original CM (O) and Weighted-CMs (W) on Amazon-Ratings (Ama), Chameleon-F (Cha), and Squirrel-F (Squ), along with the corresponding CMD values.

most of the time. This shows that CMGNN achieves more stable results by alleviating the sparsity and noise issues. As for the opposite result on Chameleon-F, this may be attributed to its small size (890 nodes), which naturally leads to unstable results.

5.4 Case Study on the Estimated CMs and CMDs

To evaluate the effectiveness of CMGNN in increasing CMD, we calculate the CMD of both original and Weighted-CMs, as illustrated in Figure 4. The results demonstrate that CMGNN is capable of enhancing the CMD across graphs with varying homophily levels, thereby resulting in better node embeddings. Even for CM with tiny CMD on Squirrel-F, CMGNN can still maintain its effectiveness.

More experimental results can be found in Appendix G, including more ablation studies, case studies on node degrees and low label rate settings, comprehensive complexity analysis, and runtime-performance tradeoff comparison.

6 Conclusion and Limitation

In this paper, we explore the underlying principle that explains the effectiveness of HTMP by investigating the connection between node discriminability and CM. We find that the effectiveness of many existing HTMP mechanisms may be credited to increasing the CMD. Inspired by this discovery, we propose CMGNN, a novel approach to enhance the CMD and node embeddings explicitly while alleviating the sparsity and noise issues. Experimental results show the effectiveness of CMGNN.

This work mainly focuses on the message-passing mechanism in existing HTGNNs under the semi-supervised setting. Thus, this paper does not analyze the other designs in HTGNNs, such as spectral- and graph-transform-based methods. Theoretical analyses and proofs are based on the CSBM-H with corresponding assumptions about node features, degrees and edges.

Acknowledgments and Disclosure of Funding

This work is supported by the National Natural Science Foundation of China (Grant No. 62476245), Zhejiang Provincial Natural Science Foundation of China (Grant No. LTGG23F030005).

References

[1] Thomas N. Kipf and Max Welling. Semi-supervised classification with graph convolutional networks. In International Conference on Learning Representations, 2017.

[2] Yanfu Zhang, Hongchang Gao, Jian Pei, and Heng Huang. Robust self-supervised structural graph neural network for social network prediction. In Proceedings of the ACM Web Conference 2022, pages 1352–1361, 2022.

[3] Xiang Wang, Xiangnan He, Meng Wang, Fuli Feng, and Tat-Seng Chua. Neural graph collaborative filtering. In Proceedings of the 42nd international ACM SIGIR conference on Research and development in Information Retrieval, pages 165–174, 2019.

[4] Xiangnan He, Kuan Deng, Xiang Wang, Yan Li, Yongdong Zhang, and Meng Wang. Lightgcn: Simplifying and powering graph convolution network for recommendation. In Proceedings

of the 43rd International ACM SIGIR conference on research and development in Information Retrieval, pages 639–648, 2020.

[5] Miller McPherson, Lynn Smith-Lovin, and James M Cook. Birds of a feather: Homophily in social networks. Annual review of sociology, 27(1):415–444, 2001.

[6] Yao Ma, Xiaorui Liu, Neil Shah, and Jiliang Tang. Is homophily a necessity for graph neural networks? In International Conference on Learning Representations, 2022.

[7] Jiong Zhu, Ryan A Rossi, Anup Rao, Tung Mai, Nedim Lipka, Nesreen K Ahmed, and Danai Koutra. Graph neural networks with heterophily. In Proceedings of the AAAI conference on artificial intelligence, volume 35, pages 11168–11176, 2021.

[8] Xin Zheng, Yixin Liu, Shirui Pan, Miao Zhang, Di Jin, and Philip S Yu. Graph neural networks for graphs with heterophily: A survey. arXiv preprint arXiv:2202.07082, 2022.

[9] Jiong Zhu, Yujun Yan, Mark Heimann, Lingxiao Zhao, Leman Akoglu, and Danai Koutra. Heterophily and graph neural networks: Past, present and future. IEEE Data Engineering Bulletin, 2023.

[10] Sami Abu-El-Haija, Bryan Perozzi, Amol Kapoor, Nazanin Alipourfard, Kristina Lerman, Hrayr Harutyunyan, Greg Ver Steeg, and Aram Galstyan. Mixhop: Higher-order graph convolutional architectures via sparsified neighborhood mixing. In international conference on machine learning, pages 21–29. PMLR, 2019.

[11] Deyu Bo, Xiao Wang, Chuan Shi, and Huawei Shen. Beyond low-frequency information in graph convolutional networks. In Proceedings of the AAAI Conference on Artificial Intelligence, volume 35, pages 3950–3957, 2021.

[12] Sitao Luan, Chenqing Hua, Qincheng Lu, Jiaqi Zhu, Mingde Zhao, Shuyuan Zhang, Xiao-Wen Chang, and Doina Precup. Revisiting heterophily for graph neural networks. Advances in neural information processing systems, 35:1362–1375, 2022.

[13] Yunchong Song, Chenghu Zhou, Xinbing Wang, and Zhouhan Lin. Ordered GNN: Ordering message passing to deal with heterophily and over-smoothing. In The Eleventh International Conference on Learning Representations, 2023.

[14] Junfu Wang, Yuanfang Guo, Liang Yang, and Yunhong Wang. Understanding heterophily for graph neural networks. In International Conference on Machine Learning, pages 50489–50529. PMLR, 2024.

[15] Sitao Luan, Chenqing Hua, Minkai Xu, Qincheng Lu, Jiaqi Zhu, Xiao-Wen Chang, Jie Fu, Jure Leskovec, and Doina Precup. When do graph neural networks help with node classification? investigating the homophily principle on node distinguishability. Advances in Neural Information Processing Systems, 36:28748–28760, 2023.

[16] Jiong Zhu, Yujun Yan, Lingxiao Zhao, Mark Heimann, Leman Akoglu, and Danai Koutra. Beyond homophily in graph neural networks: Current limitations and effective designs. Advances in neural information processing systems, 33:7793–7804, 2020.

[17] Hongbin Pei, Bingzhe Wei, Kevin Chen-Chuan Chang, Yu Lei, and Bo Yang. Geom-gcn: Geometric graph convolutional networks. In International Conference on Learning Representations, 2020.

[18] Justin Gilmer, Samuel S Schoenholz, Patrick F Riley, Oriol Vinyals, and George E Dahl. Neural message passing for quantum chemistry. In International conference on machine learning, pages 1263–1272. PMLR, 2017.

[19] Yash Deshpande, Subhabrata Sen, Andrea Montanari, and Elchanan Mossel. Contextual stochastic block models. Advances in Neural Information Processing Systems, 31, 2018.

[20] Aseem Baranwal, Kimon Fountoulakis, and Aukosh Jagannath. Graph convolution for semi-supervised classification: Improved linear separability and out-of-distribution generalization. In International Conference on Machine Learning, pages 684–693. PMLR, 2021.

[21] Rongzhe Wei, Haoteng Yin, Junteng Jia, Austin R Benson, and Pan Li. Understanding nonlinearity in graph neural networks from the bayesian-inference perspective. Advances in Neural Information Processing Systems, 35:34024–34038, 2022.

[22] Xiang Li, Renyu Zhu, Yao Cheng, Caihua Shan, Siqiang Luo, Dongsheng Li, and Weining Qian. Finding global homophily in graph neural networks when meeting heterophily. In International Conference on Machine Learning, pages 13242–13256. PMLR, 2022.

[23] Eli Chien, Jianhao Peng, Pan Li, and Olgica Milenkovic. Adaptive universal generalized pagerank graph neural network. In International Conference on Learning Representations, 2021.

[24] Yu Wang, Yuesong Shen, and Daniel Cremers. Explicit pairwise factorized graph neural network for semi-supervised node classification. In Uncertainty in Artificial Intelligence, pages 1979–1987. PMLR, 2021.

[25] Zhiqiang Zhong, Sergei Ivanov, and Jun Pang. Simplifying node classification on heterophilous graphs with compatible label propagation. Transactions on Machine Learning Research, 2022. ISSN 2835-8856.

[26] Oleg Platonov, Denis Kuznedelev, Michael Diskin, Artem Babenko, and Liudmila Prokhorenkova. A critical look at the evaluation of GNNs under heterophily: Are we really making progress? In The Eleventh International Conference on Learning Representations, 2023.

[27] Petar Veličković, Guillem Cucurull, Arantxa Casanova, Adriana Romero, Pietro Lio, and Yoshua Bengio. Graph attention networks. In The International Conference on Learning Representations, 2018.

[28] Will Hamilton, Zhitao Ying, and Jure Leskovec. Inductive representation learning on large graphs. Advances in neural information processing systems, 30, 2017.

[29] Johannes Gasteiger, Aleksandar Bojchevski, and Stephan Günnemann. Predict then propagate: Graph neural networks meet personalized pagerank. In International Conference on Learning Representations, 2019.

[30] Ming Chen, Zhewei Wei, Zengfeng Huang, Bolin Ding, and Yaliang Li. Simple and deep graph convolutional networks. In International conference on machine learning, pages 1725–1735. PMLR, 2020.

[31] Lun Du, Xiaozhou Shi, Qiang Fu, Xiaojun Ma, Hengyu Liu, Shi Han, and Dongmei Zhang. Gbk-gnn: Gated bi-kernel graph neural networks for modeling both homophily and heterophily. In Proceedings of the ACM Web Conference 2022, pages 1550–1558, 2022.

[32] Yujun Yan, Milad Hashemi, Kevin Swersky, Yaoqing Yang, and Danai Koutra. Two sides of the same coin: Heterophily and oversmoothing in graph convolutional neural networks. In 2022 IEEE International Conference on Data Mining (ICDM), pages 1287–1292. IEEE, 2022.

[33] Tao Wang, Di Jin, Rui Wang, Dongxiao He, and Yuxiao Huang. Powerful graph convolutional networks with adaptive propagation mechanism for homophily and heterophily. In Proceedings of the AAAI conference on artificial intelligence, volume 36, pages 4210–4218, 2022.

[34] Langzhang Liang, Sunwoo Kim, Kijung Shin, Zenglin Xu, Shirui Pan, and Yuan Qi. Sign is not a remedy: Multiset-to-multiset message passing for learning on heterophilic graphs. In International Conference on Machine Learning, pages 29621–29643. PMLR, 2024.

[35] Junshu Sun, Chenxue Yang, Xiangyang Ji, Qingming Huang, and Shuhui Wang. Towards dynamic message passing on graphs. In Thirty-Eighth Annual Conference on Neural Information Processing Systems, 2024.

[36] Zonghan Wu, Shirui Pan, Fengwen Chen, Guodong Long, Chengqi Zhang, and S Yu Philip. A comprehensive survey on graph neural networks. IEEE transactions on neural networks and learning systems, 32(1):4–24, 2020.

[37] Hao Chen, Yuanchen Bei, Qijie Shen, Yue Xu, Sheng Zhou, Wenbing Huang, Feiran Huang, Senzhang Wang, and Xiao Huang. Macro graph neural networks for online billion-scale recommender systems. In Proceedings of the ACM on Web Conference 2024, pages 3598–3608, 2024.

[38] Michaël Defferrard, Xavier Bresson, and Pierre Vandergheynst. Convolutional neural networks on graphs with fast localized spectral filtering. Advances in neural information processing systems, 29, 2016.

[39] Bingbing Xu, Huawei Shen, Qi Cao, Yunqi Qiu, and Xueqi Cheng. Graph wavelet neural network. In International Conference on Learning Representations, 2018.

[40] Yao Ma, Xiaorui Liu, Tong Zhao, Yozen Liu, Jiliang Tang, and Neil Shah. A unified view on graph neural networks as graph signal denoising. In Proceedings of the 30th ACM International Conference on Information & Knowledge Management, pages 1202–1211, 2021.

[41] Meiqi Zhu, Xiao Wang, Chuan Shi, Houye Ji, and Peng Cui. Interpreting and unifying graph neural networks with an optimization framework. In Proceedings of the Web Conference 2021, pages 1215–1226, 2021.

[42] Di Jin, Zhizhi Yu, Cuiying Huo, Rui Wang, Xiao Wang, Dongxiao He, and Jiawei Han. Universal graph convolutional networks. Advances in Neural Information Processing Systems, 34:10654–10664, 2021.

[43] Wei Jin, Tyler Derr, Yiqi Wang, Yao Ma, Zitao Liu, and Jiliang Tang. Node similarity preserving graph convolutional networks. In Proceedings of the 14th ACM international conference on web search and data mining, pages 148–156, 2021.

[44] Susheel Suresh, Vinith Budde, Jennifer Neville, Pan Li, and Jianzhu Ma. Breaking the limit of graph neural networks by improving the assortativity of graphs with local mixing patterns. In Proceedings of the 27th ACM SIGKDD Conference on Knowledge Discovery & Data Mining, pages 1541–1551, 2021.

[45] Chenghua Gong, Yao Cheng, Jianxiang Yu, Can Xu, Caihua Shan, Siqiang Luo, and Xiang Li. A survey on learning from graphs with heterophily: Recent advances and future directions. arXiv preprint arXiv:2401.09769, 2024.

[46] Sitao Luan, Mingde Zhao, Chenqing Hua, Xiao-Wen Chang, and Doina Precup. Complete the missing half: Augmenting aggregation filtering with diversification for graph convolutional networks. arXiv preprint arXiv:2008.08844, 2020.

[47] Yixin Liu, Zhao Li, Shirui Pan, Chen Gong, Chuan Zhou, and George Karypis. Anomaly detection on attributed networks via contrastive self-supervised learning. IEEE Transactions on Neural Networks and Learning Systems, 2021.

[48] Prithviraj Sen, Galileo Namata, Mustafa Bilgic, Lise Getoor, Brian Galligher, and Tina Eliassi-Rad. Collective classification in network data. AI magazine, 29(3):93–93, 2008.

[49] Derek Lim, Felix Hohne, Xiuyu Li, Sijia Linda Huang, Vaishnavi Gupta, Omkar Bhalerao, and Ser Nam Lim. Large scale learning on non-homophilous graphs: New benchmarks and strong simple methods. Advances in Neural Information Processing Systems, 34:20887–20902, 2021.

[50] Édouard Grave, Piotr Bojanowski, Prakhar Gupta, Armand Joulin, and Tomáš Mikolov. Learning word vectors for 157 languages. In Proceedings of the Eleventh International Conference on Language Resources and Evaluation (LREC 2018), 2018.

[51] Leskovec Jure. Snap datasets: Stanford large network dataset collection. Retrieved December 2021 from http://snap. stanford. edu/data, 2014.

[52] Benedek Rozemberczki, Carl Allen, and Rik Sarkar. Multi-scale attributed node embedding. Journal of Complex Networks, 9(2):cnab014, 2021.

[53] Jie Tang, Jimeng Sun, Chi Wang, and Zi Yang. Social influence analysis in large-scale networks. In Proceedings of the 15th ACM SIGKDD international conference on Knowledge discovery and data mining, pages 807–816, 2009.

[54] Amanda L Traud, Peter J Mucha, and Mason A Porter. Social structure of facebook networks. Physica A: Statistical Mechanics and its Applications, 391(16):4165–4180, 2012.

[55] Benedek Rozemberczki and Rik Sarkar. Twitch gamers: a dataset for evaluating proximity preserving and structural role-based node embeddings. arXiv preprint arXiv:2101.03091, 2021.

[56] Derek Lim and Austin R Benson. Expertise and dynamics within crowdsourced musical knowledge curation: A case study of the genius platform. In Proceedings of the International AAAI Conference on Web and Social Media, volume 15, pages 373–384, 2021.

[57] Jure Leskovec and Andrej Krevl. SNAP Datasets: Stanford large network dataset collection. `http://snap.stanford.edu/data`, June 2014.

[58] Jure Leskovec, Jon Kleinberg, and Christos Faloutsos. Graphs over time: densification laws, shrinking diameters and possible explanations. In Proceedings of the eleventh ACM SIGKDD international conference on Knowledge discovery in data mining, pages 177–187, 2005.

NeurIPS Paper Checklist

1. **Claims**

   Question: Do the main claims made in the abstract and introduction accurately reflect the paper's contributions and scope?

   Answer: [Yes]

   Justification: The contributions and scope of this paper are included in the abstract and introduction.

   Guidelines:

   - The answer NA means that the abstract and introduction do not include the claims made in the paper.
   - The abstract and/or introduction should clearly state the claims made, including the contributions made in the paper and important assumptions and limitations. A No or NA answer to this question will not be perceived well by the reviewers.
   - The claims made should match theoretical and experimental results, and reflect how much the results can be expected to generalize to other settings.
   - It is fine to include aspirational goals as motivation as long as it is clear that these goals are not attained by the paper.

2. **Limitations**

   Question: Does the paper discuss the limitations of the work performed by the authors?

   Answer: [Yes]

   Justification: The limitations of this work are listed in the Sec 6.

   Guidelines:

   - The answer NA means that the paper has no limitation while the answer No means that the paper has limitations, but those are not discussed in the paper.
   - The authors are encouraged to create a separate "Limitations" section in their paper.
   - The paper should point out any strong assumptions and how robust the results are to violations of these assumptions (e.g., independence assumptions, noiseless settings, model well-specification, asymptotic approximations only holding locally). The authors should reflect on how these assumptions might be violated in practice and what the implications would be.
   - The authors should reflect on the scope of the claims made, e.g., if the approach was only tested on a few datasets or with a few runs. In general, empirical results often depend on implicit assumptions, which should be articulated.

- The authors should reflect on the factors that influence the performance of the approach. For example, a facial recognition algorithm may perform poorly when image resolution is low or images are taken in low lighting. Or a speech-to-text system might not be used reliably to provide closed captions for online lectures because it fails to handle technical jargon.
- The authors should discuss the computational efficiency of the proposed algorithms and how they scale with dataset size.
- If applicable, the authors should discuss possible limitations of their approach to address problems of privacy and fairness.
- While the authors might fear that complete honesty about limitations might be used by reviewers as grounds for rejection, a worse outcome might be that reviewers discover limitations that aren't acknowledged in the paper. The authors should use their best judgment and recognize that individual actions in favor of transparency play an important role in developing norms that preserve the integrity of the community. Reviewers will be specifically instructed to not penalize honesty concerning limitations.

3. **Theory assumptions and proofs**

   Question: For each theoretical result, does the paper provide the full set of assumptions and a complete (and correct) proof?

   Answer: [Yes]

   Justification: We provide the formalization proof of Theorem 3.2 in Appendix B.

   Guidelines:

   - The answer NA means that the paper does not include theoretical results.
   - All the theorems, formulas, and proofs in the paper should be numbered and cross-referenced.
   - All assumptions should be clearly stated or referenced in the statement of any theorems.
   - The proofs can either appear in the main paper or the supplemental material, but if they appear in the supplemental material, the authors are encouraged to provide a short proof sketch to provide intuition.
   - Inversely, any informal proof provided in the core of the paper should be complemented by formal proofs provided in appendix or supplemental material.
   - Theorems and Lemmas that the proof relies upon should be properly referenced.

4. **Experimental result reproducibility**

   Question: Does the paper fully disclose all the information needed to reproduce the main experimental results of the paper to the extent that it affects the main claims and/or conclusions of the paper (regardless of whether the code and data are provided or not)?

   Answer: [Yes]

   Justification: The details of the method and experimental settings are provided in Section 4,5 and Appendix E, F.

   Guidelines:

   - The answer NA means that the paper does not include experiments.
   - If the paper includes experiments, a No answer to this question will not be perceived well by the reviewers: Making the paper reproducible is important, regardless of whether the code and data are provided or not.
   - If the contribution is a dataset and/or model, the authors should describe the steps taken to make their results reproducible or verifiable.
   - Depending on the contribution, reproducibility can be accomplished in various ways. For example, if the contribution is a novel architecture, describing the architecture fully might suffice, or if the contribution is a specific model and empirical evaluation, it may be necessary to either make it possible for others to replicate the model with the same dataset, or provide access to the model. In general. releasing code and data is often one good way to accomplish this, but reproducibility can also be provided via detailed instructions for how to replicate the results, access to a hosted model (e.g., in the case of a large language model), releasing of a model checkpoint, or other means that are appropriate to the research performed.

- While NeurIPS does not require releasing code, the conference does require all submissions to provide some reasonable avenue for reproducibility, which may depend on the nature of the contribution. For example
  (a) If the contribution is primarily a new algorithm, the paper should make it clear how to reproduce that algorithm.
  (b) If the contribution is primarily a new model architecture, the paper should describe the architecture clearly and fully.
  (c) If the contribution is a new model (e.g., a large language model), then there should either be a way to access this model for reproducing the results or a way to reproduce the model (e.g., with an open-source dataset or instructions for how to construct the dataset).
  (d) We recognize that reproducibility may be tricky in some cases, in which case authors are welcome to describe the particular way they provide for reproducibility. In the case of closed-source models, it may be that access to the model is limited in some way (e.g., to registered users), but it should be possible for other researchers to have some path to reproducing or verifying the results.

5. **Open access to data and code**

   Question: Does the paper provide open access to the data and code, with sufficient instructions to faithfully reproduce the main experimental results, as described in supplemental material?

   Answer: [Yes]

   Justification: The data and code are available in the supplementary material.

   Guidelines:

   - The answer NA means that paper does not include experiments requiring code.
   - Please see the NeurIPS code and data submission guidelines (`https://nips.cc/public/guides/CodeSubmissionPolicy`) for more details.
   - While we encourage the release of code and data, we understand that this might not be possible, so "No" is an acceptable answer. Papers cannot be rejected simply for not including code, unless this is central to the contribution (e.g., for a new open-source benchmark).
   - The instructions should contain the exact command and environment needed to run to reproduce the results. See the NeurIPS code and data submission guidelines (`https://nips.cc/public/guides/CodeSubmissionPolicy`) for more details.
   - The authors should provide instructions on data access and preparation, including how to access the raw data, preprocessed data, intermediate data, and generated data, etc.
   - The authors should provide scripts to reproduce all experimental results for the new proposed method and baselines. If only a subset of experiments are reproducible, they should state which ones are omitted from the script and why.
   - At submission time, to preserve anonymity, the authors should release anonymized versions (if applicable).
   - Providing as much information as possible in supplemental material (appended to the paper) is recommended, but including URLs to data and code is permitted.

6. **Experimental setting/details**

   Question: Does the paper specify all the training and test details (e.g., data splits, hyperparameters, how they were chosen, type of optimizer, etc.) necessary to understand the results?

   Answer: [Yes]

   Justification: The detailed experimental settings are provided in Section 5 and Appendix F.

   Guidelines:

   - The answer NA means that the paper does not include experiments.
   - The experimental setting should be presented in the core of the paper to a level of detail that is necessary to appreciate the results and make sense of them.

- The full details can be provided either with the code, in appendix, or as supplemental material.

7. **Experiment statistical significance**

   Question: Does the paper report error bars suitably and correctly defined or other appropriate information about the statistical significance of the experiments?

   Answer: [Yes]

   Justification: We report the average accuracy and the standard deviation as the performance in experiments.

   Guidelines:

   - The answer NA means that the paper does not include experiments.
   - The authors should answer "Yes" if the results are accompanied by error bars, confidence intervals, or statistical significance tests, at least for the experiments that support the main claims of the paper.
   - The factors of variability that the error bars are capturing should be clearly stated (for example, train/test split, initialization, random drawing of some parameter, or overall run with given experimental conditions).
   - The method for calculating the error bars should be explained (closed form formula, call to a library function, bootstrap, etc.)
   - The assumptions made should be given (e.g., Normally distributed errors).
   - It should be clear whether the error bar is the standard deviation or the standard error of the mean.
   - It is OK to report 1-sigma error bars, but one should state it. The authors should preferably report a 2-sigma error bar than state that they have a 96% CI, if the hypothesis of Normality of errors is not verified.
   - For asymmetric distributions, the authors should be careful not to show in tables or figures symmetric error bars that would yield results that are out of range (e.g. negative error rates).
   - If error bars are reported in tables or plots, The authors should explain in the text how they were calculated and reference the corresponding figures or tables in the text.

8. **Experiments compute resources**

   Question: For each experiment, does the paper provide sufficient information on the computer resources (type of compute workers, memory, time of execution) needed to reproduce the experiments?

   Answer: [Yes]

   Justification: We list the hardware and software resources along with the space and space complexity and run time in Appendix F and G.

   Guidelines:

   - The answer NA means that the paper does not include experiments.
   - The paper should indicate the type of compute workers CPU or GPU, internal cluster, or cloud provider, including relevant memory and storage.
   - The paper should provide the amount of compute required for each of the individual experimental runs as well as estimate the total compute.
   - The paper should disclose whether the full research project required more compute than the experiments reported in the paper (e.g., preliminary or failed experiments that didn't make it into the paper).

9. **Code of ethics**

   Question: Does the research conducted in the paper conform, in every respect, with the NeurIPS Code of Ethics `https://neurips.cc/public/EthicsGuidelines`?

   Answer: [Yes]

   Justification: The research conducted in this paper conforms, in every respect, with the NeurIPS Code of Ethics.

Guidelines:

- The answer NA means that the authors have not reviewed the NeurIPS Code of Ethics.
- If the authors answer No, they should explain the special circumstances that require a deviation from the Code of Ethics.
- The authors should make sure to preserve anonymity (e.g., if there is a special consideration due to laws or regulations in their jurisdiction).

10. **Broader impacts**

    Question: Does the paper discuss both potential positive societal impacts and negative societal impacts of the work performed?

    Answer: [Yes]

    Justification: The potential positive societal impacts are provided in Sec 1, while the potential negative societal impacts are meaningless since this work is foundational research.

    Guidelines:

    - The answer NA means that there is no societal impact of the work performed.
    - If the authors answer NA or No, they should explain why their work has no societal impact or why the paper does not address societal impact.
    - Examples of negative societal impacts include potential malicious or unintended uses (e.g., disinformation, generating fake profiles, surveillance), fairness considerations (e.g., deployment of technologies that could make decisions that unfairly impact specific groups), privacy considerations, and security considerations.
    - The conference expects that many papers will be foundational research and not tied to particular applications, let alone deployments. However, if there is a direct path to any negative applications, the authors should point it out. For example, it is legitimate to point out that an improvement in the quality of generative models could be used to generate deepfakes for disinformation. On the other hand, it is not needed to point out that a generic algorithm for optimizing neural networks could enable people to train models that generate Deepfakes faster.
    - The authors should consider possible harms that could arise when the technology is being used as intended and functioning correctly, harms that could arise when the technology is being used as intended but gives incorrect results, and harms following from (intentional or unintentional) misuse of the technology.
    - If there are negative societal impacts, the authors could also discuss possible mitigation strategies (e.g., gated release of models, providing defenses in addition to attacks, mechanisms for monitoring misuse, mechanisms to monitor how a system learns from feedback over time, improving the efficiency and accessibility of ML).

11. **Safeguards**

    Question: Does the paper describe safeguards that have been put in place for responsible release of data or models that have a high risk for misuse (e.g., pretrained language models, image generators, or scraped datasets)?

    Answer: [NA]

    Justification: This paper poses no such risk. The datasets used are all publicly available online.

    Guidelines:

    - The answer NA means that the paper poses no such risks.
    - Released models that have a high risk for misuse or dual-use should be released with necessary safeguards to allow for controlled use of the model, for example by requiring that users adhere to usage guidelines or restrictions to access the model or implementing safety filters.
    - Datasets that have been scraped from the Internet could pose safety risks. The authors should describe how they avoided releasing unsafe images.
    - We recognize that providing effective safeguards is challenging, and many papers do not require this, but we encourage authors to take this into account and make a best faith effort.

12. **Licenses for existing assets**

    Question: Are the creators or original owners of assets (e.g., code, data, models), used in the paper, properly credited and are the license and terms of use explicitly mentioned and properly respected?

    Answer: [Yes]

    Justification: The datasets and codes of baseline methods are publicly available online. We cite the original paper and mark the URL in both papers and the codebase.

    Guidelines:

    - The answer NA means that the paper does not use existing assets.
    - The authors should cite the original paper that produced the code package or dataset.
    - The authors should state which version of the asset is used and, if possible, include a URL.
    - The name of the license (e.g., CC-BY 4.0) should be included for each asset.
    - For scraped data from a particular source (e.g., website), the copyright and terms of service of that source should be provided.
    - If assets are released, the license, copyright information, and terms of use in the package should be provided. For popular datasets, `paperswithcode.com/datasets` has curated licenses for some datasets. Their licensing guide can help determine the license of a dataset.
    - For existing datasets that are re-packaged, both the original license and the license of the derived asset (if it has changed) should be provided.
    - If this information is not available online, the authors are encouraged to reach out to the asset's creators.

13. **New assets**

    Question: Are new assets introduced in the paper well documented and is the documentation provided alongside the assets?

    Answer: [Yes]

    Justification: We provide a public codebase along with an illustrative README file.

    Guidelines:

    - The answer NA means that the paper does not release new assets.
    - Researchers should communicate the details of the dataset/code/model as part of their submissions via structured templates. This includes details about training, license, limitations, etc.
    - The paper should discuss whether and how consent was obtained from people whose asset is used.
    - At submission time, remember to anonymize your assets (if applicable). You can either create an anonymized URL or include an anonymized zip file.

14. **Crowdsourcing and research with human subjects**

    Question: For crowdsourcing experiments and research with human subjects, does the paper include the full text of instructions given to participants and screenshots, if applicable, as well as details about compensation (if any)?

    Answer: [NA]

    Justification: This paper does not involve crowdsourcing nor research with human subjects.

    Guidelines:

    - The answer NA means that the paper does not involve crowdsourcing nor research with human subjects.
    - Including this information in the supplemental material is fine, but if the main contribution of the paper involves human subjects, then as much detail as possible should be included in the main paper.
    - According to the NeurIPS Code of Ethics, workers involved in data collection, curation, or other labor should be paid at least the minimum wage in the country of the data collector.

15. **Institutional review board (IRB) approvals or equivalent for research with human subjects**

    Question: Does the paper describe potential risks incurred by study participants, whether such risks were disclosed to the subjects, and whether Institutional Review Board (IRB) approvals (or an equivalent approval/review based on the requirements of your country or institution) were obtained?

    Answer: [NA]

    Justification: This paper does not involve crowdsourcing nor research with human subjects.

    Guidelines:

    - The answer NA means that the paper does not involve crowdsourcing nor research with human subjects.
    - Depending on the country in which research is conducted, IRB approval (or equivalent) may be required for any human subjects research. If you obtained IRB approval, you should clearly state this in the paper.
    - We recognize that the procedures for this may vary significantly between institutions and locations, and we expect authors to adhere to the NeurIPS Code of Ethics and the guidelines for their institution.
    - For initial submissions, do not include any information that would break anonymity (if applicable), such as the institution conducting the review.

16. **Declaration of LLM usage**

    Question: Does the paper describe the usage of LLMs if it is an important, original, or non-standard component of the core methods in this research? Note that if the LLM is used only for writing, editing, or formatting purposes and does not impact the core methodology, scientific rigorousness, or originality of the research, declaration is not required.

    Answer: [NA]

    Justification: The core method development in this paper does not involve LLMs as any important, original, or non-standard components.

    Guidelines:

    - The answer NA means that the core method development in this research does not involve LLMs as any important, original, or non-standard components.
    - Please refer to our LLM policy (`https://neurips.cc/Conferences/2025/LLM`) for what should or should not be described.

A Related Works

Homophilic Graph Neural Networks. Graph Neural Networks (GNNs) have showcased impressive capabilities in handling graph-structured data [36, 37]. Traditional GNNs are predominantly founded on the assumption of homophily, broadly categorized into two classes: spectral-based GNNs and spatial-based GNNs. *Firstly*, spectral-based GNNs acquire node representations through graph convolution operations employing diverse graph filters [1, 38, 39]. *Secondly*, spatial-based methods gather information from neighbors and update the representation of central nodes through the message-passing mechanism [27, 29, 28]. Moreover, for a more *comprehensive understanding of existing homophilic GNNs*, several unified frameworks [40, 41] have been proposed. Ma et al. [40] propose that the aggregation process in some representative homophilic GNNs can be regarded as solving a graph denoising problem with a smoothness assumption. Zhu et al. [41] establishes a connection between various message-passing mechanisms and a unified optimization problem. However, these methods have limitations, as the aggregated representations may lose discriminability when heterophilic neighbors dominate [11, 16].

Heterophilic Graph Neural Networks. Recently, some heterophilic GNNs have emerged to tackle the heterophily problem [10–13, 33, 16, 42, 43, 17, 22, 23, 44, 32, 35, 34]. *Firstly*, a commonly adopted strategy involves *expanding the neighborhood with higher homophily or richer messages*, such as high order neighborhooods [16, 42], feature-similarity-based neighborhoods [42, 43], and custom-defined neighborhoods [17, 44]. *Secondly*, some approaches [11, 33, 12, 22, 32] aim to *leverage information from heterophilic neighbors*, considering that not all heterophily is detrimental [6]. *Thirdly*, some methods [16, 10, 23, 13] adapt to heterophily by extending the combine function in message passing, creating variations for addition and concatenation.

Reviewing Heterophilic Graph Neural Networks. Heterophilic GNNs have attracted more and more research attention. Some surveys have provided a macroscopic view for reviewing heterophilic GNNs, categorizing heterophilic GNNs with shallow analysis. Specifically, Zheng et al. [8] categorizes the designs of heterophilic GNNs into non-local neighbor extensions and GNN architecture refinement. Zhu et al. [9] examines the impact of heterophilic graph characteristics on GNNs. For categorizations, it simply lists some effective designs in heterophilic GNNs. Gong et al. [45] reviews heterophilic graph learning, where message passing is only a minor aspect of its taxonomy with a broader view.

The Connection Between Message Passing and Heterophily. Recently, some efforts [6, 9, 14, 15, 46] have begun to investigate the connection between message passing and heterophily. Zhu et al. [9] highlighted that node degrees and compatibility matrices are key factors for message passing under heterophily. In ACM [12], the authors found that the performance curves of the VMP mechanism under different levels of homophily are U-shaped. Similarly, Ma et al. [6] proposed the existence of a special case of heterophily, named "good" heterophily, where the homophily ratios remain low, but the VMP mechanism can achieve strong performance. Luan et al. [15] shows that the low-pass filter works better at very low and very high homophily intervals, while the high-pass filter works better at the low to medium homophily interval. However, these works are limited in studying what kind of data is suitable for the message-passing mechanism, lacking a model-perspective understanding of heterophilic message passing.

B Proof of Theorem 3.2

To prove Theorem 3.2, we first calculate the $\text{CMD}(\mathbf{M}_{\text{CSBM-H}})$ and $\text{ENKL}(\mathbf{H}^{\text{LP}})$, respectively.

According to the definitions in CSBM-H, the corresponding compatibility matrix is as follows:

$$\mathbf{M}_{\text{CSBM-H}} = \begin{bmatrix} h, & 1-h \\ 1-h, & h \end{bmatrix}. \tag{18}$$

Thus, the corresponding CMD can be calculated by Eq.5:

$$\text{CMD}(\mathbf{M}_{\text{CSBM-H}}) = \frac{2(|h-(1-h)| + |1-h-h|)}{2} = 2|2h-1| = 4|h-\frac{1}{2}|. \tag{19}$$

On the other hand, the original $\mathbf{X}$ and LP features $\mathbf{H}^{\text{LP}} = \hat{\mathbf{A}}\mathbf{X}$ are as follows:

$$\begin{aligned} i \in \mathcal{C}_0, x_i \sim N(\boldsymbol{\mu}_0, \sigma_0^2\mathbf{I});\ h_i^{LP} \sim N(\tilde{\boldsymbol{\mu}}_0, \tilde{\sigma}_0^2\mathbf{I}), \\ j \in \mathcal{C}_1, x_j \sim N(\boldsymbol{\mu}_1, \sigma_1^2\mathbf{I});\ h_j^{LP} \sim N(\tilde{\boldsymbol{\mu}}_1, \tilde{\sigma}_1^2\mathbf{I}), \end{aligned} \tag{20}$$

where $\tilde{\boldsymbol{\mu}}_0 = h(\boldsymbol{\mu}_0 - \boldsymbol{\mu}_1) + \boldsymbol{\mu}_1$, $\tilde{\boldsymbol{\mu}}_1 = h(\boldsymbol{\mu}_1 - \boldsymbol{\mu}_0) + \boldsymbol{\mu}_0$, $\tilde{\sigma}_0^2 = \frac{h(\sigma_0^2-\sigma_1^2)+\sigma_1^2}{d_0}$, $\tilde{\sigma}_1^2 = \frac{h(\sigma_1^2-\sigma_0^2)+\sigma_0^2}{d_1}$.
Considering the formula of ENKL Eq.2, we first calculate $d^2_{\mathbf{H}^{\text{LP}}}$.

$$\begin{aligned}
d^2_{\mathbf{X}} &= \|\boldsymbol{\mu}_0 - \boldsymbol{\mu}_1\|_2^2, \\
d^2_{\mathbf{H}^{\text{LP}}} &= \|\tilde{\boldsymbol{\mu}}_0 - \tilde{\boldsymbol{\mu}}_1\|_2^2 \\
&= \|h(\boldsymbol{\mu}_0 - \boldsymbol{\mu}_1) + \boldsymbol{\mu}_1 - (h(\boldsymbol{\mu}_1 - \boldsymbol{\mu}_0) + \boldsymbol{\mu}_0)\|_2^2 \\
&= \|(2h-1)(\boldsymbol{\mu}_0 - \boldsymbol{\mu}_1)\|_2^2 \\
&= (2h-1)^2 d^2_{\mathbf{X}}.
\end{aligned} \tag{21}$$

In CSBM-H, $F_h = 2$, we further assume $d_0 = d_1 = d$, that is, ignoring the influence of node degrees. Now we have $\tilde{\sigma}_0^2 = \frac{h(\sigma_0^2-\sigma_1^2)+\sigma_1^2}{d}$ and $\tilde{\sigma}_1^2 = \frac{h(\sigma_1^2-\sigma_0^2)+\sigma_0^2}{d}$.
The ENKL of LP feature is as follows:

$$\begin{aligned}
\text{ENKL}(\mathbf{H}^{\text{LP}}) &= -d^2_{\mathbf{H}^{\text{LP}}}\left(\frac{1}{4\tilde{\sigma}_1^2} + \frac{1}{4\tilde{\sigma}_0^2}\right) - \frac{2}{4}\left(\frac{\tilde{\sigma}_0^2}{\tilde{\sigma}_1^2} + \frac{\tilde{\sigma}_1^2}{\tilde{\sigma}_0^2} - 2\right) \\
&= 1 - (2h-1)^2 d^2_{\mathbf{X}}\left(\frac{d}{4[h(\sigma_1^2-\sigma_0^2)+\sigma_0^2]} + \frac{d}{4[h(\sigma_0^2-\sigma_1^2)+\sigma_1^2]}\right) \\
&\quad - \frac{1}{2}\left(\frac{h(\sigma_0^2-\sigma_1^2)+\sigma_1^2}{h(\sigma_1^2-\sigma_0^2)+\sigma_0^2} + \frac{h(\sigma_1^2-\sigma_0^2)+\sigma_0^2}{h(\sigma_0^2-\sigma_1^2)+\sigma_1^2}\right) \\
&= 1 - (2h-1)^2 d^2_{\mathbf{X}} \cdot \frac{(\sigma_0^2+\sigma_1^2)d}{4\left[-(\sigma_0^2-\sigma_1^2)^2h^2 + (\sigma_0^2-\sigma_1^2)^2h + \sigma_0^2\sigma_1^2\right]} \\
&\quad - \frac{1}{2} \cdot \frac{2(\sigma_0^2-\sigma_1^2)^2h^2 - 2(\sigma_0^2-\sigma_1^2)^2h + \sigma_0^4 + \sigma_1^4}{-(\sigma_0^2-\sigma_1^2)^2h^2 + (\sigma_0^2-\sigma_1^2)^2h + \sigma_0^2\sigma_1^2} \\
&= 1 + d^2_{\mathbf{X}} \cdot d \cdot \frac{(\sigma_0^2+\sigma_1^2)(h^2-h+\frac{1}{4})}{(\sigma_0^2-\sigma_1^2)^2h^2 - (\sigma_0^2-\sigma_1^2)^2h - \sigma_0^2\sigma_1^2} \\
&\quad + \frac{(\sigma_0^2-\sigma_1^2)^2h^2 - (\sigma_0^2-\sigma_1^2)^2h + \frac{1}{2}\sigma_0^4 + \frac{1}{2}\sigma_1^4}{(\sigma_0^2-\sigma_1^2)^2h^2 - (\sigma_0^2-\sigma_1^2)^2h - \sigma_0^2\sigma_1^2} \\
&= 1 + \frac{d^2_{\mathbf{X}} \cdot d(\sigma_0^2+\sigma_1^2)}{(\sigma_0^2-\sigma_1^2)^2} \cdot \frac{h^2-h+\frac{1}{4}}{h^2-h-\frac{\sigma_0^2\sigma_1^2}{(\sigma_0^2-\sigma_1^2)^2}} + \frac{h^2-h+\frac{\sigma_0^4+\sigma_1^4}{2(\sigma_0^2-\sigma_1^2)^2}}{h^2-h-\frac{\sigma_0^2\sigma_1^2}{(\sigma_0^2-\sigma_1^2)^2}} \\
&= \frac{d^2_{\mathbf{X}} \cdot d(\sigma_0^2+\sigma_1^2)}{(\sigma_0^2-\sigma_1^2)^2} \cdot \frac{\frac{1}{4}+\frac{\sigma_0^2\sigma_1^2}{(\sigma_0^2-\sigma_1^2)^2}}{(h-\frac{1}{2})^2-\frac{1}{4}-\frac{\sigma_0^2\sigma_1^2}{(\sigma_0^2-\sigma_1^2)^2}} + \frac{\frac{\sigma_0^4+\sigma_1^4}{2(\sigma_0^2-\sigma_1^2)^2}+\frac{\sigma_0^2\sigma_1^2}{(\sigma_0^2-\sigma_1^2)^2}}{(h-\frac{1}{2})^2-\frac{1}{4}-\frac{\sigma_0^2\sigma_1^2}{(\sigma_0^2-\sigma_1^2)^2}} \\
&\quad + \frac{d^2_{\mathbf{X}} \cdot d(\sigma_0^2+\sigma_1^2)}{(\sigma_0^2-\sigma_1^2)^2} + 2 \\
&= \frac{d^2_{\mathbf{X}} \cdot d(\sigma_0^2+\sigma_1^2)}{(\sigma_0^2-\sigma_1^2)^2} \cdot \frac{\frac{(\sigma_0^2+\sigma_1^2)^2}{4(\sigma_0^2-\sigma_1^2)^2}}{(h-\frac{1}{2})^2-\frac{(\sigma_0^2+\sigma_1^2)^2}{4(\sigma_0^2-\sigma_1^2)^2}} + \frac{\frac{(\sigma_0^2+\sigma_1^2)^2}{2(\sigma_0^2-\sigma_1^2)^2}}{(h-\frac{1}{2})^2-\frac{(\sigma_0^2+\sigma_1^2)^2}{4(\sigma_0^2-\sigma_1^2)^2}} \\
&\quad + \frac{d^2_{\mathbf{X}} \cdot d(\sigma_0^2+\sigma_1^2)}{(\sigma_0^2-\sigma_1^2)^2} + 2 \\
&= \left[\frac{d^2_{\mathbf{X}} \cdot d(\sigma_0^2+\sigma_1^2)}{(\sigma_0^2-\sigma_1^2)^2} + 2\right] \cdot \left[\frac{\frac{(\sigma_0^2+\sigma_1^2)^2}{4(\sigma_0^2-\sigma_1^2)^2}}{(h-\frac{1}{2})^2-\frac{(\sigma_0^2+\sigma_1^2)^2}{4(\sigma_0^2-\sigma_1^2)^2}} + 1\right].
\end{aligned} \tag{22}$$

Since $\boldsymbol{\mu}_0, \boldsymbol{\mu}_1, \sigma_0^2, \sigma_1^2$ and d are fixed parameters in CSBM-H when only considering the change of homophily h, we simplify the above formulation by new variables a, b.

$$\begin{aligned}
a &= \left[\frac{d^2_{\mathbf{X}} \cdot d(\sigma_0^2+\sigma_1^2)}{(\sigma_0^2-\sigma_1^2)^2} + 2\right] \in [2, +\infty), \\
b &= \frac{(\sigma_0^2+\sigma_1^2)^2}{4(\sigma_0^2-\sigma_1^2)^2} \in [\frac{1}{4}, +\infty).
\end{aligned} \tag{23}$$

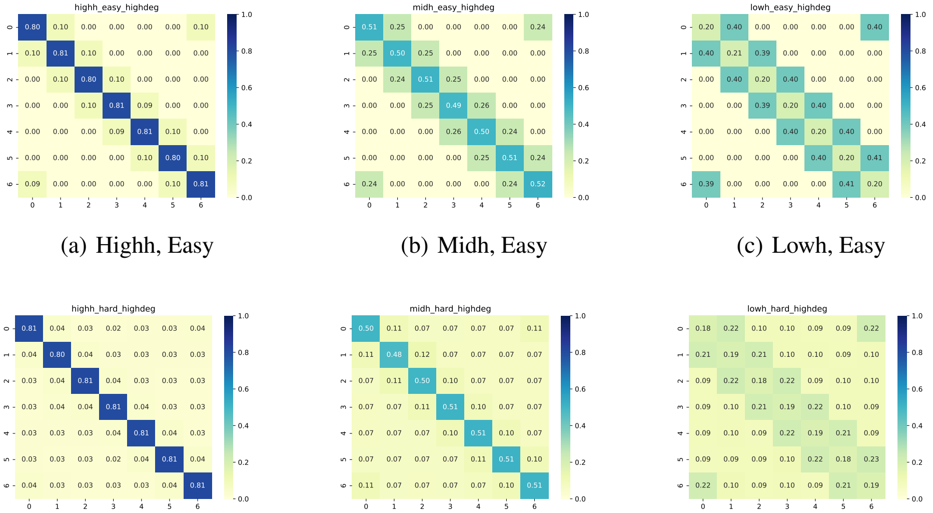

(a) Highh, Easy

(b) Midh, Easy

(c) Lowh, Easy

(d) Highh, Hard

(e) Midh, Hard

(f) Lowh, Hard

Figure 5: The visualization of the compatibility matrix on synthetic graphs.

Thus, the ENKL can be represented as follows:

$$\mathrm{ENKL}(\mathbf{H}^{\mathrm{LP}}) = a\left[\frac{b}{(h-\frac{1}{2})^2 - b} + 1\right]. \tag{24}$$

Furthermore, let $t = |h - \frac{1}{2}| \in [0, \frac{1}{2}]$ since $h \in [0, 1]$, the CMD and ENKL can be represented as follows:

$$\begin{aligned} \mathrm{CMD}(\mathbf{M}_{\text{CSBM-H}}) &= 4t, \\ \mathrm{ENKL}(\mathbf{H}^{\mathrm{LP}}) &= \frac{ab}{t^2 - b} + a. \end{aligned} \tag{25}$$

To simplify the computation, we analyze monotonicity with the aid of derivatives.

$$\begin{aligned} \frac{d\mathrm{CMD}}{dt} &= 4 > 0, \\ \frac{d\mathrm{ENKL}}{dt} &= \frac{-2abt}{(t^2 - b)^2} \le 0. \end{aligned} \tag{26}$$

That means CMD increases monotonically with t, while ENKL decreases monotonically with t. Thus, the covariance between CMD and ENKL is negative: $\mathrm{Cov}(\mathrm{CMD}(\mathbf{M}_{\text{CSBM-H}}), \mathrm{ENKL}(\mathbf{H}^{\mathrm{LP}})) < 0$.

C The Experiments on Synthetic Datasets

To explore the performance impact of homophily level, node degrees, and compatibility matrix (CMs) on simple GNNs, we conduct some experiments on synthetic datasets.

C.1 Synthetic Datasets

We construct synthetic graphs considering the factors of homophily, CMs, and degrees. For homophily, we set 3 levels including Lowh (0.2), Midh (0.5), and Highh (0.8). For CMs, we set two levels of discriminability, including Easy and Hard. For degrees, we set two levels, including Lowdeg (4) and Highdeg (18). Note that with a certain homophily level, we can only control the non-diagonal elements of CMs. Thus, there are a total of 12 synthetic graphs following the above settings. These synthetic graphs are based on the Cora dataset, which provides node features and labels, which means, only the edges are constructed. We visualize the CMs of these graphs in Figure 5. Since there is no

Table 5: Node classification accuracy of GCN on synthetic datasets.

Factors	Highh, Easy	Highh, Hard	Midh, Easy	Midh, Hard	Lowh, Easy	Lowh, Hard
Highd	99.15 ± 0.35	99.48 ± 0.24	86.42 ± 4.13	90.52 ± 1.05	89.34 ± 2.19	39.22 ± 2.34
Lowd	89.98 ± 1.59	91.25 ± 0.85	70.85 ± 1.59	70.20 ± 1.41	56.46 ± 2.63	40.91 ± 1.75

significant difference in CMs between low-degree and high-degree, we only plot the high-degree ones. Further, the edges are randomly constructed under the guidance of these CMs and degrees to form the synthetic graphs.

C.2 Experiments on Synthetic Datasets

We use GCN to analyze the performance impact of the above factors. The semi-supervised node classification performance of GCN is shown in Table 5 while the baseline performance of MLP (72.54 ± 2.18) is the same among these datasets since their difference is only on edges. From these results, we have some observations: (1) High homophily is not necessary, **GCN can also work well on low homophily but discriminative CM**; (2) Low degrees have a negative impact on performance, especially when the CMs are relatively less discriminative. This also indicates that nodes with lower degrees are more likely to have confused semantic neighborhoods; (3) When handling nodes with confused semantic neighborhoods, GCN may contaminate central nodes with their neighborhoods' messages, which leads to worse performance than MLP. This once again reminds us of the importance of enhancing the CM discriminability.

D The Posterior Evaluation about the Weighted-CM and CMD in HTGNNs

In this part, we give the details of the empirical posterior evaluation on GloGNN [22], GPR-GNN [23], and ACM-GCN [12].

GloGNN. GloGNN learns a global pair-wise coefficient matrix $\mathbf{Z}$ and utilizes it as the aggregation weights during message passing. Thus, we directly calculate this matrix as the practical aggregate weights matrix $\dot{\mathbf{A}}^{glo} = \mathbf{Z}$, then regard $\dot{\mathbf{A}}$ as the neighborhood and calculate the Weighted-CM and its corresponding CMD.

ACM-GCN. ACM-GCN merges messages from various filters using adaptive weights, effectively altering edge weights to construct the Weight-CM with optional negative elements due to the high-pass filter. Thus, we leverage the learned weights to rebuild a practical aggregate weights matrix $\dot{\mathbf{A}}^{acm}$ based on the low-pass filter $\hat{\mathbf{A}}$ and high-pass filter $\mathbf{I} - \hat{\mathbf{A}}$, then regard $\dot{\mathbf{A}}^{acm}$ as the neighborhood and calculate the Weighted-CM and its corresponding CMD.

GPRGNN. GPR-GNN integrates the CMs of multiple-order neighborhoods with adaptive weights to form a more discriminative Weighted-CM. Thus, we utilize the learned weights to rebuild a practical aggregate weights matrix $\dot{\mathbf{A}}^{gpr}$ based on the multi-hop adjacency matrices $[\mathbf{I}, \mathbf{A}, \mathbf{A}^2, ..., \mathbf{A}^k]$, then regard $\dot{\mathbf{A}}^{gpr}$ as the neighborhood and calculate the Weighted-CM and its corresponding CMD.

The visualization of Weighted-CMs and corresponding CMD on various datasets can be seen in Figure 6.

E Additional Detailed Implementation of CMGNN

Considering the influence of node degree in compatibility matrix estimation. As mentioned in Section 3, the semantic neighborhood of low-degree nodes may display inconsistencies with CM. Thus, nodes with low degrees deserve low weights during the CM estimation. We manually set up a weighting function range in $[0, 1]$:

$$w_i^d = \begin{cases} d_i/2K, & d_i \leq K, \\ 0.25 + d_i/4K, & K < d_i \leq 3K, \\ 1, & otherwise. \end{cases} \tag{27}$$

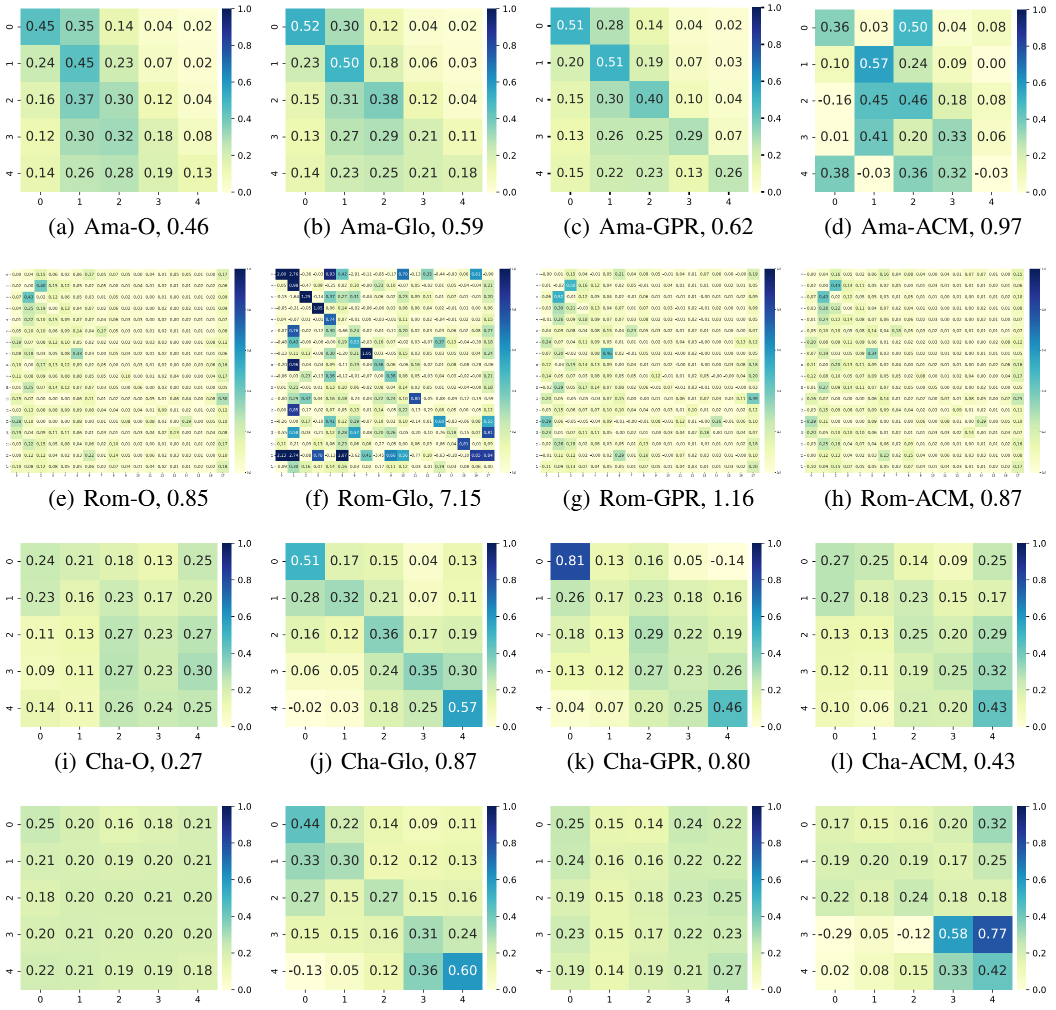

(a) Ama-O, 0.46 (b) Ama-Glo, 0.59 (c) Ama-GPR, 0.62 (d) Ama-ACM, 0.97

(e) Rom-O, 0.85 (f) Rom-Glo, 7.15 (g) Rom-GPR, 1.16 (h) Rom-ACM, 0.87

(i) Cha-O, 0.27 (j) Cha-Glo, 0.87 (k) Cha-GPR, 0.80 (l) Cha-ACM, 0.43

(m) Squ-O, 0.08 (n) Squ-Glo, 0.81 (o) Squ-GPR, 0.10 (p) Squ-ACM, 0.94

Figure 6: Visualizations of Weighted-CMs and CMD of GloGNN, GPR-GNN, and ACM-GCN on various datasets.

For low-degree nodes, increases in degree should yield more significant benefits compared to high-degree nodes. Beyond a certain threshold, increases in degree yield tiny benefits. We have empirically chosen K and $3K$ as fixed thresholds for the weighting function to simplify the design without multiple attempts. This approach is straightforward and can be substituted with other forms that meet the same criteria. In practice, the compatibility matrix is estimated considering the various node degrees:

$$\hat{\mathbf{M}} = \text{Norm}((\mathbf{w}^d \cdot \mathbf{g} \cdot \hat{\mathbf{C}})^T)\mathbf{C}^{nb}. \tag{28}$$

The utilization of additional structural features. In line with existing methods [12, 22], we treat the topology structure as additional node features. These features, shown as the adjacency matrix $\mathbf{A}$, depict node connections. Each row $\mathbf{A}_i$ can be viewed as an extra N-dimensional feature of node i. Thus, the input representation of the first layer can be obtained in two ways:

$$\mathbf{Z}^0 = [\mathbf{X}\mathbf{W}^X \| \hat{\mathbf{A}}\mathbf{W}^A]\mathbf{W}^0, \text{ or } \mathbf{Z}^0 = \mathbf{X}\mathbf{W}^0. \tag{29}$$

Specifically, (i) using additional features, where $\mathbf{W}^X \in \mathbb{R}^{d_f \times d_r}$, $\mathbf{W}^A \in \mathbb{R}^{N \times d_r}$ and $\mathbf{W}_0 \in \mathbb{R}^{2d_r \times d_r}$ are learnable matrices; (ii) using only attribute features, where $\mathbf{W}^0 \in \mathbb{R}^{d_f \times d_r}$, where d_r is the dimension of node embeddings.

Message COMBNIE with Adaptive Weights. The aggregated messages from node ego, raw, and supplementary neighborhoods are $\mathbf{Z}^l_{ego}$, $\mathbf{Z}^l_{raw}$ and $\mathbf{Z}^l_{sup}$, respectively. The combination weights are

Algorithm 1 Algorithm of CMGNN

```
Require: Graph $\mathcal{G} = (\mathcal{V}, \mathcal{E}, \mathbf{X}, \mathbf{A}, \mathbf{Y})$, loss weight $\lambda$, epoch $E$
Ensure: Predicted labels $\hat{\mathbf{Y}}$
Initialize the soft predicted labels $\tilde{C}$ with other elements $\frac{1}{K}$.
Construct class prototypes as additional virtual neighbors for all nodes via Eq.9.
for iteration 1, 2, ..., $E$ do
    Obtain the input representations for the first layer via Eq.29.
    Estimate the compatibility matrix via Eq.10, Eq.11, Eq.27, and Eq.28.
    Obtain the output representations through the CM-aware message-passing mechanism via
    Eq.13, Eq.14, and Eq.15.
    Obtain the predicted logits (soft label) $\tilde{\mathbf{C}}$ via Eq.16.
    Calculate loss $\mathcal{L}$ via Eq.17.
    Back-propagation $\mathcal{L}$ to optimize the weights of networks.
    if the performance in the validation set improved then
        update the compatibility matrix with current soft predicted label $\tilde{\mathbf{C}}$.
    end if
end for
Obtain the predicted labels $\hat{\mathbf{Y}}$ via $\hat{\mathbf{Y}} = \text{Softmax}(\tilde{\mathbf{C}})$.
output $\hat{\mathbf{Y}}$
```

learned by an MLP with Softmax:

$$[\alpha^l_{ego}, \alpha^l_{raw}, \alpha^l_{sup}] = \text{Softmax}(\text{Sigmoid}([\mathbf{Z}^l_{ego} \| \mathbf{Z}^l_{raw} \| \mathbf{Z}^l_{sup} \| \mathbf{d}]\mathbf{W}^l_{att})\mathbf{W}^l_{mix}), \tag{30}$$

where $\mathbf{W}^l_{att} \in \mathbb{R}^{(3d_r+1)\times 3}$ and $\mathbf{W}^l_{mix} \in \mathbb{R}^{3\times 3}$ are two learnable weight matrixes, $\mathbf{d}$ is the node degrees which may be helpful to weights learning.

The Message Passing of Class Prototypes. Specifically, the virtual prototype nodes are viewed as additional nodes, which have the same message-passing mechanism as real nodes:

$$\begin{aligned} \mathbf{Z}^{ptt,l} &= \text{diag}(\alpha^{ptt,l}_{ego})\mathbf{Z}^{ptt,l-}\mathbf{W}^l_{ego} + \text{diag}(\alpha^{ptt,l}_{raw})\hat{\mathbf{A}}^{ptt}\mathbf{Z}^{ptt,l-1}\mathbf{W}^l_{raw} \\ &+ \text{diag}(\alpha^{ptt,l}_{sup})(\mathbf{A}^{ptt,sup} \odot \mathbf{B}^{ptt,sup})\mathbf{Z}^{ptt,l-1}\mathbf{W}^l_{sup}, \\ \mathbf{Z}^{ptt} &= \mathop{\Big\|}_{l=0}^{L} \mathbf{Z}^{ptt,l}, \end{aligned} \tag{31}$$

where $\mathbf{A}^{sup,ptt} = \mathbf{1} \in \mathbb{R}^{K\times K}$ and $\mathbf{B}^{sup,ptt} = \hat{\mathbf{C}}^{ptt}\hat{\mathbf{M}}$ are similar with those of real nodes.

F More Details about the Experimental Settings

In this section, we describe the details of the new benchmarks, including (i) the reason why we need a new benchmark: drawbacks of existing datasets; (ii) detailed descriptions of newly organized datasets; (iii) baseline methods and the codebase; (iv) details of obtaining benchmark performance; and (v) detailed experimental settings of CMGNN.

F.1 Drawbacks in Existing Datasets

Existing works mostly follow the settings and datasets used in Pei et al. [17], including 6 heterophilic datasets (Cornell, Texas, Wisconsin, Actor, Chameleon, and Squirrel) and 3 homophilic datasets (Cora, Citeseer, and Pubmed). Platonov et al. [26] pointed out serious data leakages in Chameleon and Squirrel, while Cornell, Texas, and Wisconsin are too small with very imbalanced classes. Further, we revisit other datasets and discover new drawbacks: (i) In the ten splits of Citeseer, there are two inconsistent ones, which have smaller training, validation, and test sets that could cause issues with statistical results; (ii) Cora's data split ratios are inconsistent with the expected ones. These drawbacks may lead to certain issues in the conclusions of previous works.

Therefore, to build a comprehensive and fair benchmark for model effectiveness evaluation, we newly organize 13 datasets with unified splitting across various homophily values and scales.

F.2 Newly Organized Datasets

In our benchmark, we adopt ten different types of publicly available datasets with a unified splitting setting (48%/32%/20% for training/validation/testing) for fair model comparison, including **Roman-Empire** [26], **Amazon-Ratings** [26], **Chameleon-F** [26], **Squirrel-F** [26], **Actor** [17], **Flickr** [47], **BlogCatalog** [47], **Pubmed** [48], **Penn94** [49], **Twitch-Gamer** [49], **Genius** [49], **Pokec** [49] and **Snap-Patents** [49]. The datasets have a variety of homophily values from low to high. The statistics and splitting of these datasets are shown in Table 6. The detailed description of the datasets is as follows:

Table 6: Statistics and splitting of the experimental benchmark datasets.

Dataset	Nodes	Edges	Attributes	Classes	Avg. Degree	Undirected	Homophily	Train / Valid / Test
Roman-Empire	22,662	65,854	300	18	2.9	✓	0.05	10,877 / 7,251 / 4,534
Amazon-Ratings	24,492	186,100	300	5	7.6	✓	0.38	11,756 / 7,837 / 4,899
Chameleon-F	890	13,584	2,325	5	15.3	✗	0.25	427 / 284 / 179
Squirrel-F	2,223	65,718	2,089	5	29.6	✗	0.22	1,067 / 711 / 445
Actor	7,600	30,019	932	5	3.9	✗	0.22	3,648 / 2,432 / 1,520
Flickr	7,575	479,476	12,047	9	63.3	✓	0.24	3,636 / 2,424 / 1,515
BlogCatalog	5,196	343,486	8,189	6	66.1	✓	0.40	2,494 / 1,662 / 1,040
Pubmed	19,717	88,651	500	3	4.5	✓	0.80	9,463 / 6,310 / 3,944
Penn94	41,554	1,362,229	5	2	65.6	✗	0.47	19,945 / 13,297 / 8,312
Twitch-Gamer	168,114	6,797,557	7	2	40.4	✗	0.55	80,694 / 53,796 / 33,624
Genius	421,961	984,979	12	2	2.3	✗	0.62	202,541 / 135,027 / 84,393
Pokec	1,632,803	30,622,564	65	2	18.8	✗	0.45	783,667 / 522,444 / 326,529
Snap-Patents	2,923,922	13,975,788	269	5	4.8	✗	0.07	1,403,482 / 935,655 / 584,785

- **Roman-Empire**[2] [26] is derived from the extensive article on the Roman Empire found on the English Wikipedia, chosen for its status as one of the most comprehensive entries on the platform. It contains 22,662 nodes and 65,854 edges between nodes. Each node represents an individual word from the text, with the total number of nodes mirroring the length of the article. An edge between two nodes is established under one of two conditions: the words are sequential in the text or they are linked in the sentence's dependency tree, indicating a grammatical relationship where one word is syntactically dependent on the other. Consequently, the graph is structured as a chain graph, enriched with additional edges that represent these syntactic dependencies. It encompasses a total of 18 distinct node classes, with each node being equipped with 300-dimensional attributes obtained by fastText word embeddings [50].
- **Amazon-Ratings**[2] [26] is sourced from the Amazon product co-purchasing network metadata dataset [51]. It contains 24,492 nodes and 186,100 edges between nodes. The nodes within this graph represent products, encompassing a variety of categories such as books, music CDs, DVDs, and VHS video tapes. An edge between nodes signifies that the respective products are often purchased together. The objective is to forecast the average rating assigned to a product by reviewers, with the ratings being categorized into five distinct classes. For the purpose of node feature representation, we have utilized the 300-dimensional mean values derived from fastText word embeddings [50], extracted from the textual descriptions of the products.
- **Chameleon-F** and **Squirrel-F**[2] [26] are specialized collections of Wikipedia page-to-page networks [52], of which the data leakage nodes are filtered out by Platonov et al. [26]. Within these datasets, each node symbolizes a web page, and edges denote the mutual hyperlinks that connect them. The node features are derived from a selection of informative nouns extracted directly from Wikipedia articles. For the purpose of classification, nodes are categorized into five distinct groups based on the average monthly web traffic they receive. Specifically, Chameleon-F contains 890 nodes and 13,584 edges between nodes, with each node being equipped with 2,325-dimensional features. Squirrel-F contains 2,223 nodes and 65,718 edges between nodes, with each node being equipped with a 2,089-dimensional feature vector.
- **Actor**[3] [17] is an actor-centric induced subgraph derived from the broader film-director-actor-writer network, as originally presented by Tang et al. [53]. In this refined network, each node corresponds to an individual actor, and the edges signify the co-occurrence of these actors on the same Wikipedia page. The node features are identified through the presence of certain keywords found within

[2] `https://github.com/yandex-research/heterophilous-graphs/tree/main/data`

[3] `https://github.com/bingzhewei/geom-gcn/tree/master/new_data/film`

the actors' Wikipedia entries. For the purpose of classification, the actors are organized into five distinct categories based on the words of the actor's Wikipedia. Statistically, it contains 7,600 nodes and 30,019 edges between nodes, with each node being equipped with a 932-dimensional feature vector.

- **Flickr** and **Blogcatalog**[4] [47] are two datasets of social networks, originating from the blog-sharing platform BlogCatalog and the photo-sharing platform Flickr, respectively. Within these datasets, nodes symbolize the individual users of the platforms, while links signify the followship relations that exist between them. In the context of social networks, users frequently create personalized content, such as publishing blog posts or uploading and sharing photos with accompanying tag descriptions. These textual contents are consequently treated as attributes associated with each node. The classification objective is to predict the interest group of each user. Specifically, Flickr contains 7,575 nodes and 479,476 edges between nodes. The graph encompasses a total of 9 distinct node classes, with each node being equipped with a 12047-dimensional attribute vector. BlogCatalog contains 5,196 nodes and 343,486 edges between nodes. The graph encompasses a total of 6 distinct node classes, with each node being equipped with 8189-dimensional attributes.
- **Pubmed**[5] [48] is a classical citation network consisting of 19,717 scientific publications with 44,338 links between them. The text contents of each publication are treated as its node attributes, and thus each node is assigned a 500-dimensional attribute vector. The target is to predict which of the paper categories each node belongs to, with a total of 3 candidate classes.
- **Penn94**[6] [49] is a friendship network derived from the Facebook 100 networks, featuring university students from 2005 [54]. In this network, each node represents a student and is labeled with the user's reported gender. The node features include major, second major or minor, dorm or house, year, and high school.
- **Twitch-Gamer**[6] [49] is a subgraph from the streaming platform Twitch, with nodes representing users and edges connecting mutual followers [55]. Node features encompass the number of views, creation and update dates, language, lifetime, and account status. The task is to predict whether a channel contains explicit content.
- **Genius**[6] [49] is a subnetwork extracted from genius.com, a website for crowdsourced annotations of song lyrics [56]. In this graph, nodes represent users, and edges connect users who follow each other. User features include expertise scores, contribution counts, roles, and more. Some users are labeled as "gone", indicating a higher likelihood of being spam accounts. Our goal is to predict whether a user is marked as "gone".
- **Pokec**[6] [49] is a friendship graph from a Slovak online social network, with nodes representing users and edges indicating directed friendship relations [57]. Node features are derived from profile information, such as geographical region, registration time, and age. The task is to classify users based on their gender.
- **Snap-Patents**[6] [49] is a U.S. patent network, where nodes correspond to patents and edges denote citation relationships [58]. Node features are derived from patent metadata. The task is to classify patents into five categories based on the time of their grant.

F.3 Baseline Methods and the Codebase

For comprehensive comparisons, we choose 20 representative baseline methods as in the benchmark, which can be categorized into four main groups of works as follows:

(i) **Shallow Model**: MLP;

(ii) **Homopihlous Graph Neural Networks**: GCN [1], GAT [27], GraphSAGE [28], APPNP [29], and GCNII [30];

(iii) **Heterophilous Graph Neural Networks**: H2GCN [16], MixHop [10], GBK-GNN [31], GGCN [32], GloGNN [22], HOGGCN [33], GPR-GNN [23], ACM-GCN [12], OrderedGNN [13], M2MGNN [45], and N^2 [34];

(iv) **Compatibility Matrix-based Models**: CLP [25], EPFGNN [24], and CPGNN [7].

[4] `https://github.com/TrustAGI-Lab/CoLA/tree/main/raw_dataset`

[5] `https://linqs.soe.ucsc.edu/datac`

[6] `https://github.com/CUAI/Non-Homophily-Large-Scale/tree/master/data`

To explore the performance of baseline methods on newly organized datasets and facilitate future expansions, we collect the official/reproduced codes from GitHub and integrate them into a unified codebase. Specifically, all methods share the same data loaders and evaluation metrics. One can easily run different methods with only parameters changing within the codebase. The codebase is based on the widely used PyTorch[7] framework, supporting both DGL[8] and PyG[9]. Detailed usage of the codebase is available in the Readme file of the codebase.

F.4 Details of Obtaining Benchmark Performance

Following the settings in existing methods, we construct 10 random splits (48%/32%/20% for train/valid/test) for each dataset and report the average performance among 10 runs on them, along with the standard deviation. For all baseline methods except MLP, GCN, and GAT, we conduct parameter searches within the search space recommended by the original papers. The searches are based on the NNI framework with an annealing strategy. We use Adam as the optimizer for all methods. Each method has dozens of search trails according to their time costs, and the best performances are reported. The currently known optimal parameters of each method are listed in the codebase. We run these experiments on NVIDIA GeForce RTX 3090 GPUs with 24G memory. The out-of-memory error during model training is reported as OOM in Table 2 and 3.

F.5 Detailed Experimental Settings of CMGNN

CMGNN has the same experimental settings within the benchmark, including datasets, splits, evaluations, hardware, optimizer, and so on.

Parameters Search Space. We list the search space of parameters in Table 7, where patience is for the maximum epoch early stopping, n_hidden is the embedding dimension of hidden layers as well as the representation dimension d_r, relu_varient decides ReLU applying before message aggregation or not as in Luan et al. [12], structure_info determines whether to use structure information as supplement node features or not.

Table 7: Parameter search space of our method.

Parameters	Range
learning rate	{0.001, 0.005, 0.01, 0.05}
weight_decay	{0, 1e-7, 5e-7, 1e-6, 5e-6, 5e-5, 5e-4}
patience	{200, 400}
dropout	[0, 0.9]
λ	{0, 0.01, 0.1, 1, 10}
layers	{1, 2, 4, 8}
n_hidden	{32, 64, 128, 256}
relu_variant	{True, False}
structure_info	{True, False}

G More Details about Experiments

In this section, we show some additional experimental results and analyses.

G.1 Detailed Analysis about the comparison between CMGNN and existing CM-based methods

Specifically, CMGNN achieves better performance and benefits from the approach of utilizing CM in the following aspects: (i) Better robustness for low-quality pseudo labels: Existing CM-based methods utilize CM to guide the weights of propagation, which can lead to error accumulation with

[7] `https://pytorch.org`

[8] `https://www.dgl.ai`

[9] `https://www.pyg.org`

Table 8: Ablation study results (%) on the effects of additional structural features, where True denotes CMGNN with additional structural features and False denotes CMGNN with only node features.

Structural Features	Roman-Empire	Amazon-Ratings	Chameleon-F	Squirrel-F	Actor	Flickr	BlogCatalog	Pubmed
True	68.43 ± 2.23	**52.13 ± 0.55**	**45.70 ± 4.92**	**41.89 ± 2.34**	35.72 ± 0.75	**92.66 ± 0.46**	96.47 ± 0.58	88.90 ± 0.45
False	**84.35 ± 1.27**	51.41 ± 0.57	44.85 ± 5.64	40.49 ± 1.55	**36.82 ± 0.78**	92.05 ± 0.75	**97.00 ± 0.52**	**89.99 ± 0.32**

Table 9: Node classification accuracy comparison (%) among nodes with different degrees.

Dataset	**Amazon-Ratings**					**Flickr**					**BlogCatalog**				
Deg. Prop.(%)	0∼20	20∼40	40∼60	60∼80	80∼100	0∼20	20∼40	40∼60	60∼80	80∼100	0∼20	20∼40	40∼60	60∼80	80∼100
CMGNN	**59.78**	**58.36**	**53.08**	41.74	47.86	**92.56**	**91.19**	92.71	**93.24**	93.65	**94.13**	**97.17**	**98.29**	**97.99**	**97.47**
ACM-GCN	57.35	56.21	51.74	41.55	46.47	90.44	91.17	**92.85**	93.19	89.50	92.17	96.68	97.83	97.84	96.51
OrderedGNN	56.32	56.16	51.20	**41.85**	**50.26**	86.48	90.07	92.40	92.79	93.40	92.19	96.09	97.48	97.36	96.27
GCNII	50.61	49.94	47.49	**41.85**	47.76	87.49	90.54	92.29	92.68	**95.09**	92.81	96.73	97.58	97.90	97.43
Dataset	**Roman-Empire**					**Chameleon-F**					**Actor**				
Deg. Prop.(%)	0∼20	20∼40	40∼60	60∼80	80∼100	0∼20	20∼40	40∼60	60∼80	80∼100	0∼20	20∼40	40∼60	60∼80	80∼100
CMGNN	**88.60**	**87.00**	**85.59**	**86.25**	**74.33**	40.73	**45.28**	**56.02**	**46.64**	39.93	35.56	37.14	38.40	36.03	36.84
ACM-GCN	79.00	77.87	73.52	72.09	53.77	39.51	41.21	52.25	45.80	**47.09**	34.48	36.58	36.27	34.63	**37.46**
OrderedGNN	**88.60**	**87.00**	85.56	84.68	69.69	**43.21**	44.51	49.16	38.27	32.23	35.94	**38.06**	37.87	35.77	37.15
GCNII	86.79	85.14	85.20	84.75	71.09	34.84	42.56	47.50	40.45	41.84	**36.89**	37.20	**38.53**	**38.02**	36.99
Dataset	**Squirrel**					**Pubmed**									
Deg. Prop.(%)	0∼20	20∼40	40∼60	60∼80	80∼100	0∼20	20∼40	40∼60	60∼80	80∼100					
CMGNN	**45.37**	**47.10**	**45.25**	**34.86**	37.10	89.32	89.33	89.31	**92.62**	**89.39**					
ACM-GCN	41.12	44.30	44.22	32.97	**42.10**	89.60	**89.54**	89.58	92.02	89.23					
OrderedGNN	43.78	45.53	43.09	27.90	28.48	89.67	89.37	89.45	92.54	89.02					
GCNII	43.08	45.55	43.65	33.07	38.05	**89.77**	89.50	89.24	92.45	88.86					

inaccurate pseudo labels. This is a common limitation of CM-based methods. In CMGNN, the CM is used to construct desired messages while original neighborhoods are preserved, mitigating the impact of inaccurate pseudo labels. (ii) Unlock the effectiveness of CM for low-degree nodes: Existing CM-based methods redefine pair-wise relations only for existing edges, limiting the effectiveness of CMs for low-degree nodes. In CMGNN, virtual neighbors can provide prototype messages from every class, enhancing neighborhood messages for low-degree or even isolated nodes. (iii) More accurate estimation of CM: While existing CM-based methods take naive approaches to estimate or initialize CM, CMGNN considers the effects of node degrees and model prediction confidence, resulting in more accurate CM estimation, especially in real-world situations. Additionally, CM in CMGNN is continuously updated with more accurate pseudo labels, creating a positive cycle.

G.2 Ablation study on additional structural features

Utilizing additional structural features is a common approach in heterophilous GNNs that offers another way to use connection relationships, introducing both discriminant and redundant information. Thus, it presents a trade-off between the advantages and disadvantages. We conducted an ablation study to examine its effects and report the results in Table 8. The additional structure features have positive effects on four datasets, while others have negative effects. It doesn't significantly impact performance except for Roman-Empire. Moreover, CMGNN can still achieve competitive results without using additional structural features.

G.3 Performance on Nodes with Various Levels of Degrees

To verify the effect of CMGNN on low-degree nodes, we divide the test set nodes into 5 parts according to their degrees and report the classification accuracy respectively. We compare CMGNN with 3 top-performance methods and show the results in Table 9. In general, nodes with low degrees tend to have incomplete and noisy semantic neighborhoods. Thus, our outstanding performances on the top 20% nodes with the least degree demonstrate the effectiveness of CMGNN for providing supplementary neighborhood messages. Further, we can find that OrderedGNN and GCNII are good at dealing with nodes with high degrees, while ACM-GCN is relatively good at nodes with low degrees. And CMGNN , to a certain extent, can be adapted to both situations at the same time.

Table 10: Performance comparison on low-label rate setting.

Method	Roman-Empire	Amazon-Ratings	Chameleon-F	Pubmed
MLP	58.14±1.40	37.03±0.43	36.74±2.97	83.07±0.55
GCN	33.53±0.77	37.32±0.52	36.91±2.22	83.95±0.62
GCNII	63.27±0.72	39.93±0.87	38.40±3.27	**86.04±0.74**
ACM-GCN	59.93±2.03	39.96±0.81	37.43±2.84	85.54±0.79
OrderedGNN	64.76±2.20	40.00±0.90	38.91±2.57	85.59±0.68
CMGNN	**65.93±2.17**	**40.02±0.86**	**40.11±2.82**	**85.62±0.94**

G.4 Performance on low label rate setting

We conduct an experiment to investigate the performance of CMGNN under the low label rate setting. The label rate for training is set as 5% to meet the low label rate setting, and the datasets include Roman-Empire, Amazon-Ratings, Chameleon-F, and Pubmed. We compare CMGNN with 2 base and 3 top-performance baseline methods, including MLP, GCN, GCNII, ACMGCN, and OrderedGNN. The classification accuracy comparison is as Table 10. Consistent with the main results, CMGNN can also achieve outstanding performance on the low label rate setting, demonstrating the effectiveness of CMGNN on handling the noise issue.

G.5 Visualization of Weighted-CM and CMD of CMGNN

We visualize the original and Weighted-CM of CMGNN along with the corresponding CMDs in Figure 7. Obviously, CMGNN has increased the CMDs with Weighted-CMs. This shows that even with incomplete node labels, CMGNN can estimate and enhance high-quality CMs that provide valuable neighborhood information to nodes. Meanwhile, it can adapt to graphs with various levels of heterophily.

G.6 Efficiency Study

Complexity Analysis. The number of learnable parameters in layer l of CMGNN is $3d_r(d_r+1)+9$, compared to $d_r d_r$ in GCN and $3d_r(d_r+1)+9$ in ACM-GCN, where d_r is the dimension of representations. The time complexity of layer l is composed of three parts:

(i) AGGREGATE: $O(N{d_r}^2)$, $O(N{d_r}^2+Md_r)$ and $O(N{d_r}^2+NKd_r)$ for node ego, raw neighborhood and the sufficient neighborhood respectively, where N and $M=|\mathcal{E}|$ denotes the number of nodes and edges;

(ii) COMBINE: $O(3N(3d_r+1)+12N)$ for calculating adaptive weights and $O(3N)$ for combination;

(iii) Final: $O(1)$ for concatenations.

Thus, the overall time complexity of L-layer CMGNN is $O(L(Nd_r(3d_r+K+9)+Md_r+18N)+1)$, or $O(LN{d_r}^2+LMd_r)$ for brevity.

Experimental Running Time. We report the actual average running time (ms per epoch) of baseline methods and CMGNN in Table 11 for comparison. The results demonstrate that CMGNN can balance both performance effectiveness and running efficiency.

Trade-off Analysis between Effectiveness and Efficiency. We have also visualized the trade-off between performance accuracy and empirical runtime compared to baseline methods in Figure 8. From the results, we can see that CMGNN achieves the best performance with relatively low time consumption. Compared with OrderedGNN and GCNII, which have the second- and third-best average ranks, CMGNN offers both better accuracy and lower time consumption.

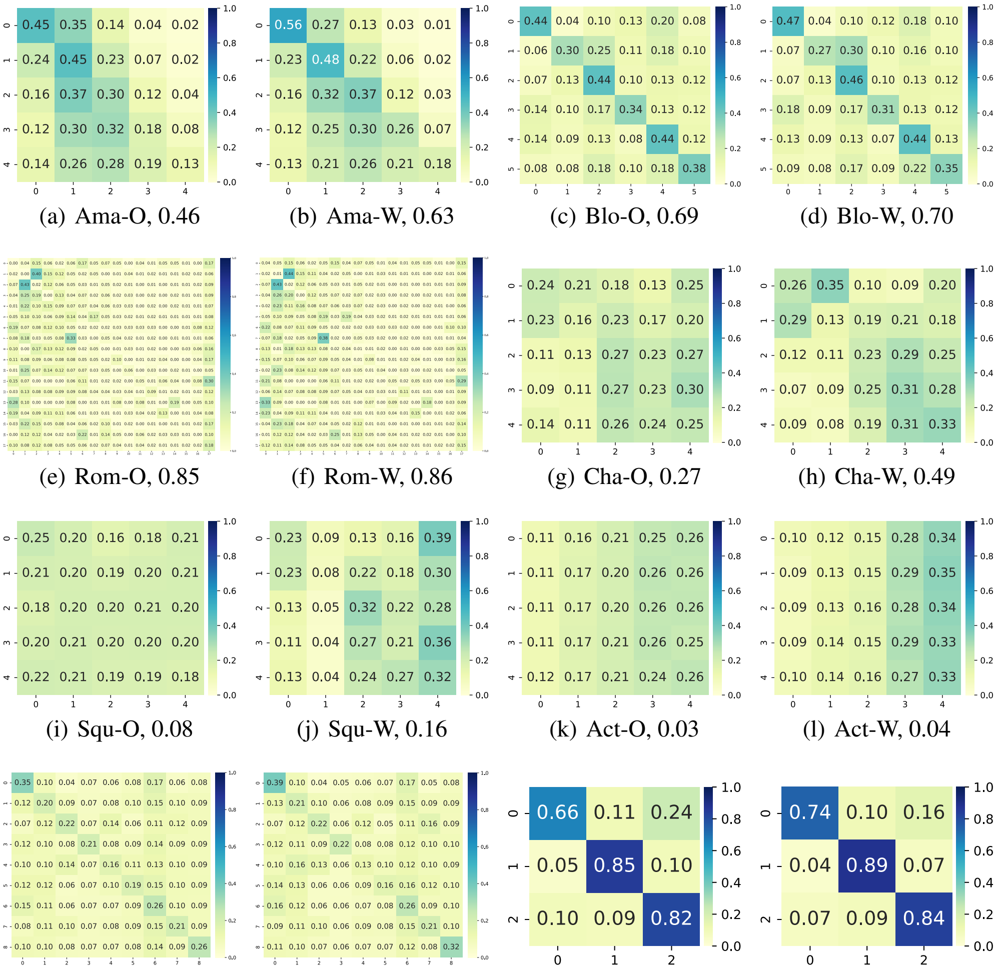

(a) Ama-O, 0.46 (b) Ama-W, 0.63 (c) Blo-O, 0.69 (d) Blo-W, 0.70

(e) Rom-O, 0.85 (f) Rom-W, 0.86 (g) Cha-O, 0.27 (h) Cha-W, 0.49

(i) Squ-O, 0.08 (j) Squ-W, 0.16 (k) Act-O, 0.03 (l) Act-W, 0.04

(m) Fli-O, 0.40 (n) Fli-W, 0.44 (o) Pub-O, 1.40 (p) Pub-W, 1.51

Figure 7: The visualization of original (O) and Weighted-CM (W) of CMGNN along with the CMDs on all small-scale datasets.

Table 11: Efficiency study results of average model running time (ms/epoch). OOM denotes an out-of-memory error during the model training.

Method	Roman-Empire	Amazon-Ratings	Chameleon-F	Squirrel-F	Actor	Flickr	BlogCatalog	Pubmed
MLP	7.8	7.0	6.1	6.5	6.3	9.1	6.7	6.1
GCN	33.8	33.4	7.9	20.6	34.4	37.2	30.4	35.6
GAT	15.9	67.3	10.3	14.0	30.8	66.2	17.6	33.4
APPNP	14.6	15.9	13.9	21.3	14.6	20.2	23.2	21.2
GCNII	29.4	28.4	37.3	19.6	37.7	84.2	97.6	258.0
CPGNN	12.7	20.3	12.2	13.4	13.6	18.9	16.7	14.0
H2GCN	20.0	31.2	17.2	32.4	55.6	415.7	165.5	39.0
MixHop	434.6	486.3	21.9	31.0	30.6	90.4	81.6	89.5
GBK-GNN	119.8	191.8	31.0	238.1	157.9	OOM	OOM	137.0
GGCN	OOM	OOM	55.7	42.1	199.8	111.2	108.7	2290.8
GloGNN	25.4	19.3	121.8	23.3	1292	562.9	30.9	43.2
HOGGCN	OOM	OOM	25.2	54.3	1002.9	707.3	367.4	OOM
GPR-GNN	15.9	12.5	22.3	23.2	16.7	15.9	14.7	13.2
ACM-GCN	56.7	56.7	26.1	29.7	22.5	60.7	31.7	37.1
OrderedGNN	86.0	110.8	49.5	60.1	67.8	107.0	88.3	88.1
M2MGNN	275.6	84.3	52.7	169.1	400.2	136.7	220.5	151.0
N^2	236.8	184.4	172.0	160.6	134.5	191.2	116.5	184.9
CMGNN	51.5	93.5	62.5	64.7	19.0	52.5	69.8	102.9

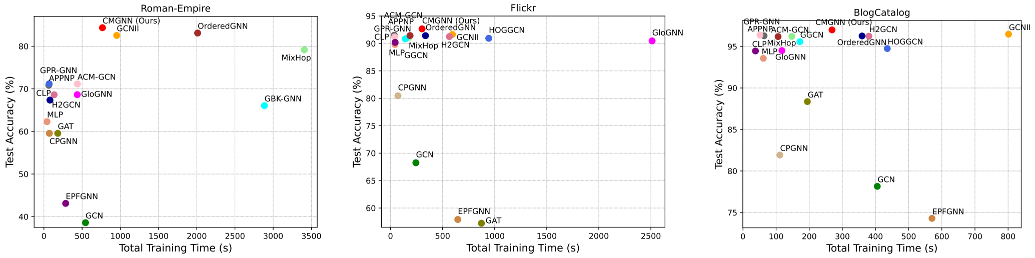

(a) Roman-Empire

(b) Flickr

(c) Blogcatalog

Figure 8: Visualizations of the trade-off between performance accuracy and training time compared with baseline methods on three representative datasets.